MATCHING A CHELATOR (DOTA) WITH IONS FOR RADIO-PHARMACEUTICAL APPLICATIONS USING DFT STUDY

EBENEZER KWABENA FRIMPONG

215068623

UNIVERSITY OF
KWAZULU-NATAL

INYUVESI
YAKWAZULU-NATALI

Submitted in fulfillment of the requirements for the degree of Masters in Pharmaceutical Sciences in the School of Health Science, University of KwaZulu-Natal

Supervisors

Dr Bahareh Honarparvar

Dr Adam A. Skelton

December 2016

MATCHING A CHELATOR (DOTA) WITH IONS FOR RADIO-PHARMACEUTICAL APPLICATIONS USING DFT STUDY

EBENEZER KWABENA FRIMPONG

215068623

2016

A dissertation submitted to the School of Health Sciences, College of Health Science, University of KwaZulu-Natal, Westville, for the degree of Master of Pharmaceutical Sciences.

This is a dissertation by manuscript with an overall introduction and final summary.

This is to certify that the content of this dissertation is the original research work of Mr. Ebenezer Kwabena Frimpong, supervised by:

Supervisor: Signed: ----------------------Name: **Dr B. Hornarparvar Date: ………………**

Co-Supervisor: Signed: ------------------Name: **Dr A.A. Skelton   Date: ………………..**

DECLARATION

I, Mr. **Ebenezer Kwabena Frimpong**, declare as follows:

1.   That the work defined in this dissertation has not been submitted to UKZN or any other tertiary institution for purposes of obtaining an academic qualification, whether by myself or any other party.

2.   That my contribution to the project was as follows:

• The research reported in this dissertation, except where otherwise indicated, is my original work

• This dissertation does not contain other person's data, pictures, graphs or other information, unless specifically acknowledged as being sourced from other persons.

3.   This dissertation does not comprise other person's writing, unless specifically acknowledged as being sourced from other researchers. Where other written sources have been quoted, then:

• Their words have been re-written but the general information attributed to them has been referenced.

• Where their exact words have been used, then their writing has been placed in italics, inside quotation marks and duly referenced.

Signed:

EK. Frimpong

Student Number 215068623

Date: 12/12/2016

DEDICATION

This work is dedicated to my parents Mr and Mrs Frimpong who gave me the peradventure to get education.

ACKNOWLEDGEMENTS

LIST OF PUBLICATIONS

Publications in peer review journals included in this thesis

Ebenezer Frimpong, Adam A. Skelton, Bahareh Honarparvar, DFT Study of the Interactions between DOTA Chelator and Competitive Alkali Metal Ions, *Tetrahedron.* Under review.

Contributions:

Ebenezer Frimpong ran the project, carried out all calculations and wrote the paper as the main author.

B. Honarparvar and A. A. Skelton – Supervisors

Ebenezer Frimpong, Adam A. Skelton, Bahareh Honarparvar. Non-covalent interactions between DOTA as a bifunctional chelator with radiometal ions for radiolabeling: A DFT study, under submission.

Contributions:

Ebenezer Frimpong ran the project, carried out all calculations and wrote the paper as the main author.

B. Honarparvar and A. A. Skelton – Supervisors

OTHER RESEARCH OUTPUT

Conference: International AIDS society official volunteer scientific poster presentation section, 21st International AIDS Conference (18-22 July 2016), Durban, SA

Workshop: Certificate of participation Center for High performance computing (CHPC) in conjunction with University of Kwa Zulu Natal (UKZN) AMBER workshop with renowned software developers Ross Walker (University of California, San Diego) and Adrian Roitberg (University of Florida) January,2016, Westville Campus, Durban

TABLE OF CONTENTS

LIST OF FIGURES

Chapter 1

Chapter 2

Chapter 3

interacting with the selected radiometal ions are marked by dotted lines. '**A**': DOTA—Cu^{2+} and DOTA—Ga^{3+} have 4N and 2O in close proximity with ions. '**B**': DOTA—In^{3+} and DOTA—Sc^{3+} have 4N and 4O atoms within (≤ 2.5 Å) range. Carbonyl oxygen (O^C) are in close contact with an ion. Nitrogen and carbonyl oxygen atoms are in close contact with an ion (N). Nitrogen is in close contact with an ion but carbonyl oxygen is not in close proximity (N^*).

LIST OF TABLES

Chapter 1

Chapter 2

APPENDICES

CHAPTER 2

Table S1. Absolute translational entropies (cal mol^{-1} K^{-1}) for free ions and DOTA—ion complexes obtained by B3LYP/6-311G+(2d,2p) and Def2-TPVZ basis set for Rb$^+$.   63

Table S2. The average interatomic distances (Å) between ions and N, O atoms of DOTA (≤3.5 Å), within 3-arm conformations of DOTA—alkali metal complexes, obtained by the DFT/B3LYP method with 6-311 G+ (2d, 2p) basis set and Def2-TPVZ for Rb$^+$.   63

Table S3. Natural atomic charges of ions, within 3-arm conformations of DOTA—alkali metal complexes, obtained by B3LYP/6-311+G(2d,2p) and Rb$^+$ (Def2-TPVZ).   64

CHAPTER 3

Table S1. Absolute translational entropies (cal mol^{-1} K^{-1}) for free ions and DOTA—ion complexes obtained by B3LYP/6-311G+(2d,2p) and DGDPVZ basis set for ions.   65

Table S2. Natural atomic charges of ions, within 3-arm conformations of DOTA—radiometal complexes, obtained by B3LYP/6-311+G(2d,2p) and DGDPVZ basis set for ions.   65

LIST OF ABBREVIATIONS AND ACRONYMS

AO	Atomic orbitals
B3LYP	Becke,3-Parameter,Lee-Yang-Parr
BFC	Bifunctional chelator
CBDO2A	4,10-bis(carboxy-methyl)-1,4,7,10-tetraazabicyclo[5.5.2]tetradecane
CBTE2A	4,11-bis(carboxymethyl)-1,4,8,11-tetraazabicyclo[6.6.2]hexadecane
CPCM	Conductor-like Polarizable Continuum Model
CHX-A"-DTPA	CHX-A"-diethylenepentaacetic acid
Def2-TZVPD	Def2-triple zeta valence polarized with one diffused function
DFT	Density Functional Theory
DGDZVP	Density Gauss Double Zeta Valence Polarized basis set
DOTA	1, 4, 7, 10-tetraazacyclododecane-1, 4, 7, 10-tetraacetic acid
EA	Electron Affinity
ECP	Effective Core Potential
GUI	Graphical User Interface
HOMO	Highest Occupied Molecular Orbital
HPLC	High Performance Liquid Chromatography
IP	Ionization Potential
LANL2DZ	Los Alamos natural laboratory 2-double -Z
LP	Lone Pair
LUMO	Lowest Unoccupied Molecular Orbital
MEP	Minimum Energy Path
MRI	Magnetic Resonance Imaging
NAC	Natural Atomic Charge
NBO	Natural Bond Orbital
NOTA	1,4,7-triazacyclononane-triacetic acid
PES	Potential Energy Surface

PET	Positron Emission Tomography
QM	Quantum Mechanics
SCRF	Self-consistent reaction field
SMD	Solvation Model
SPECT	Single Photon Emission Computed Tomography
TETA	1,4,8,11-tetraazacyclotetradecane-N,N',N'',N'''-tetraacetic acid
TLC	Thin Layer Chromatography
ωB97XD	Dispersion density functional

ABSTRACT

Organometallic chelators can be potentially used for radiometal-based pharmaceuticals. The bifunctional chelator, which is covalently bound to a lead compound, forms a stable chelator—ion complex to deliver an isotope, as a labelling agent, towards a specific *in vivo* target. The quest to find the optimal match between chelators and radiometal ions is of interest in the field of radio pharmaceuticals. A loss of radiometal ion from a chelator without reaching to its specific target organ *in vivo* could be disastrous to the body. The present project is focused on the complexation of 1, 4, 7, 10-tetraazacyclododecane-1, 4, and 7, 10-tetraacetic acid (DOTA) with alkali metals and radiometal ions. Herein, we investigated DOTA—alkali metal ions complexes with density functional theory using B3LYP and ωB97XD functionals and the 6-311+G(2d,2p) basis set for Li^+, Na^+ and K^+ and Def2-TZVPD for Rb^+. Conformational possibilities, starting from x-ray crystal structures and considering a different number of arms (2, 3 and 4) interacting with the ions were explored. Interaction and relaxation energies, thermochemical parameters, HOMO/LUMO energies, $\Delta E_{HOMO\text{-}LUMO}$ and chemical hardness indicate the decrease in the stability of DOTA—ions down the alkali metal series. Natural bond orbital analysis reveals charge transfer between DOTA and alkali metals. Regarding radiometal ions, the geometries for the various complexes were consistent with experimentally reported binding constants. NBO analysis indicates charge transfer from the chelator to the radio metals resulting in reduced positive atomic charge values for all the ions. DOTA—Ga^{3+}, DOTA—In^{3+} and DOTA—Sc^{3+} complexes recorded higher $\Delta E_{LUMO\text{-}HOMO}$ energies and chemical hardness values. The DOTA—Cu^{2+} complex was the least stable among the selected complexes. This study serves as a guide to researchers in the field of organometallic chelators, particularly; radio-pharmaceuticals in finding the efficient optimal match between chelators and different metal ions.

CHAPTER 1

INTRODUCTION

1.1   Chelation and chelator types: Acyclic and macrocyclic

The importance of the chelation process in science is enormous and cannot be overlooked. Research has revealed that the technological applications of chelators and the chelation process have been widely embraced in our industries. Chelator binds a radiometal ion to release an isotope to a specific target organ *in vivo* [1]. Diethylenetriaminopentaacetic acid (DTPA) was synthesized by Frost for the first time[2]. Complexation of DTPA and its derivatives with radio metals (^{111}In, ^{213}Bi, $^{86/90}$Y, ^{177}Lu, 99mTc and $^{67/68}$Ga) are used in the field of medicine. DTPA derivatives are preferred over DOTA regarding radiomettalation of monoclonal antibodies. CHX-A"-DTPA is used for radio immunotherapy [3-5]. For the labelling of biomolecules with 99mTc acyclic chelators are mostly applied. The labeling reactions were performed using required temperatures, tetra amine based ligands with 99mTc gave good results against all other chelators. They formed a good complex showing high kinetic inertness [6-11].

DOTA, NOTA, TETA and CB-TE2A with Ga^{3+}, In^{3+}, Y^{3+}, Lu^{3+} and Cu^{2+} ions used for the radiometallation of peptides improve, the pharmacokinetics of radiopharmaceuticals[12]. CB-TE2A derivatives have been developed lately to solve the high blood concentration of DOTA and TETA complexes with copper [13-16]. NOTA is a hexa-dentate N_3O_3 chelator. NOTA complexes with $^{67/68}$Ga and $^{64/67}$Cu are more stable [17, 18].

Thermodynamic stability of their radiometal complexes make the macrocyclic chelators a preferred choice than acyclic chelators. These chelators are more kinetically inert to dissociation. Macrocyclic chelator experienced reduction in entropic loss during its co-ordination. Significant decrease in entropic loss associated with acyclic chelators make it thermodynamically unfavorable [19-24].

1.2   DOTA

Stetter and Frank reported synthesis of DOTA in 1976[25]. DOTA (1, 4, 7, 10-tetra acetic acid) is a twelve-membered tetraaza macro cycle (**Figure 1**) which contains four pendant carboxylate arms connected, to cyclen amines. It is a bifunctional chelator (BFC). One terminus co-ordinates a radio metal ion and the other holds, a bioactive molecule during its operations. DOTA complexes show

high kinetic stability. In medical resonance imaging (MRI), DOTA-ligands are employed as contrasting agents for the treatment of cancer. DOTA is the potential chelator used for the preparation of lanthanide radiopharmaceuticals for therapeutic purposes [26] and form stable complexes with these ions: $^{67/68}$Ga, ^{111}In, $^{86/90}$Y and $^{64/67}$Cu [27-34].
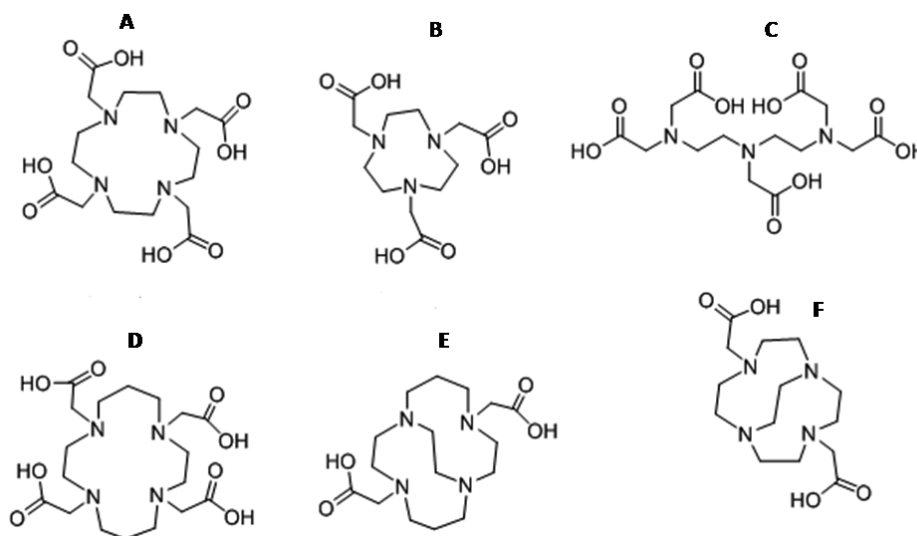
Figure 1. Commonly used chelators. **A**: Molecular structure of DOTA; **B**: Molecular structure of NOTA, **C**: Molecular structure of TETA; **E**: Molecular structure of CB-TE2A; **F**: Molecular structure of CB-DO2A.

1.3   Significance of our study in radio-pharmaceutical applications

The loss of radiometal ions from a chelator without reaching its target organ *in vivo*, in the presence of these biological competitive ions (Na$^+$ and K$^+$) is one of the main setbacks in radiopharmaceuticals. Finding the optimal match between a chelator and radiometal ions is of great importance to researchers. It is notable that alkali metal ions found in body have the capacity to compete with radiometals coordinated with DOTA for therapeutic and diagnosis of diseases which could affect, radiolabeling efficiency of the chelator. Quantum mechanical calculations were performed to study the interactions between DOTA and alkali metal ions to compare their stabilities in aqueous and vacuum and that of chelator—radiometal ions complexes.

1.4   Co-ordination chemistry of DOTA with radiometal ions based on crystallographic data

Distorted octahedral structure (coordination number 6) has been reported for DOTA and copper complex (**Figure 2A**) [35]. Hexa-coordinated structure (distorted octahedral) between DOTA and

Ga (III) was reported in 2006 (**Figure 2B**) [36]. Bombieri *et al* reported an octa-coordinated square prismatic geometry exhibited by Single crystal of [Sc(DOTA)] ⁻ (**Figure 2C**)[37]. Indium forms a robust complex with DOTA (**Table 1**). There is no reported crystallographic data available for In (III) and DOTA complex other than its amide-armed derivatives In (III) of P-amino amide (**Figure 2D**) which shows twisted (~28˚) square anti-prismatic geometry (**Figure 2D**)[38, 39].
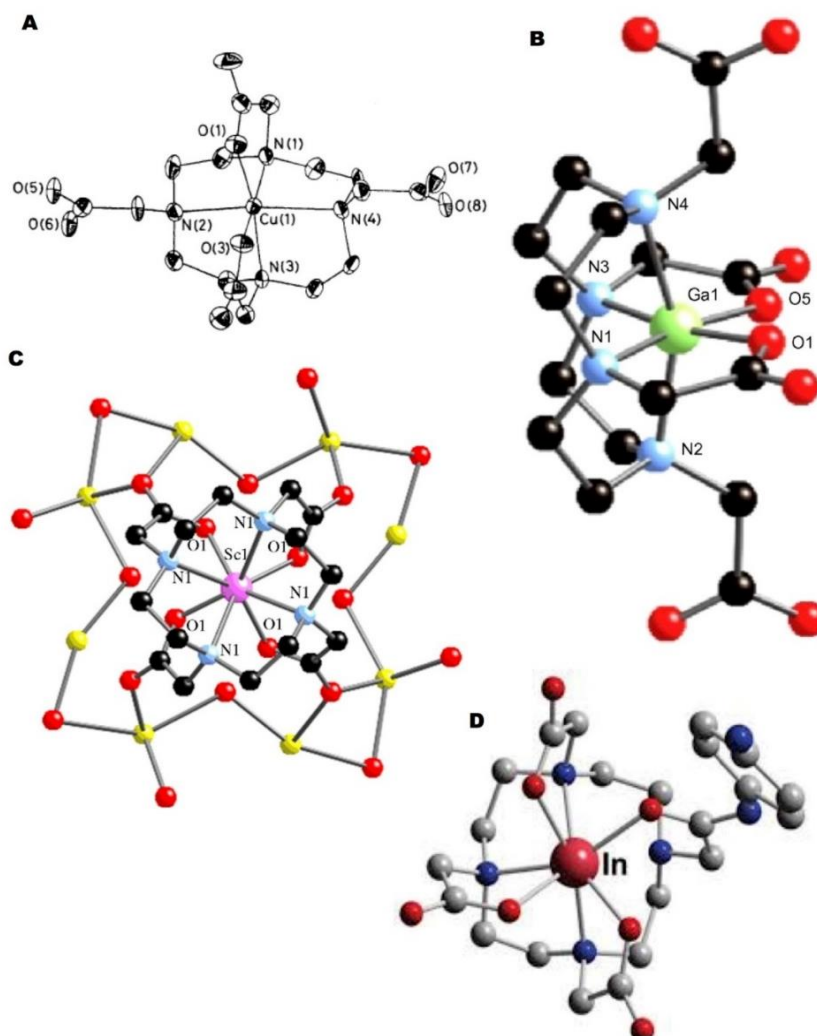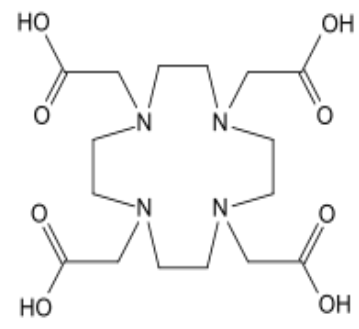
Figure 2. Molecular structures of **A**: Cu_2 (DOTA).$5H_2O$; **B:** [Ga (HDOTA).$5.5H_2O$]; **C:** 3(Na [Sc (DOTA)]).$18H_2O$; **D:** In (III) complex of P-aminoanilide**.**

Table 1. Experimental data obtained for DOTA complexed with radiometal ions[1].

	Radiometal ions	Radiolabeling conditions	$LogK_{ML}$	Geometry
  DOTA, 1,4,7,10-tetraazacyclododecane1,4,7,10-tetraacetic acid, maximum CN = 8, donor set N_4O_4	$^{64}Cu^{2+}$	25–90 1C, 30–60 min, pH 5.5–6.5	22.2, 22.7	Distorted octahedron
	$^{67/68}Ga^{3+}$	37–90 1C, 10–30 min, pH 4.0–5.5	21.3 (pM 15.2, 18.5)	Distorted octahedron
	$^{44/47}Sc^{3+}$	95 1C, 20–30 min, pH 4.0	27.0 (pM 26.5)	Square antiprism
	$^{111}In^{3+}$	37–100 1C, 15–60 min, pH 4.0–6.	23.9 (pM 17.8–18.8)	**Square antiprism

**No known x-ray structure available for this complex.

1.5 Radiopharmaceuticals

Radiopharmaceuticals are drugs that consist of two components: a radionuclide that transmits the mechanism of action through its decay and a targeting, biomolecule or organic ligand that reveals the localization of the radio pharmaceutical and their route of administration mainly through intravenous injection.

1.5.1 Therapeutic

They release ionizing (radiation) to affected targets in our bodies. Availability of therapeutic isotopes and finding its exact location in diseased tissues is the main challenge in the field of radiotherapy [40].

Figure 3. Radionuclides in medicine. Different colors refer to the radiations they emmit as indicated on top of the figure.

1.5.2   Diagnostic radiopharmaceuticals

A diagnostic radiopharmaceutical employ gamma-emitting isotope for single photon emission computed tomography (SPECT) or a positron-emitting isotope for positron emission tomography (PET). Low concentrations (10^{-6} – 10^{-8} M) preferred for its operation. It is significant to point out that it should not have any pharmacological effects [41-47].
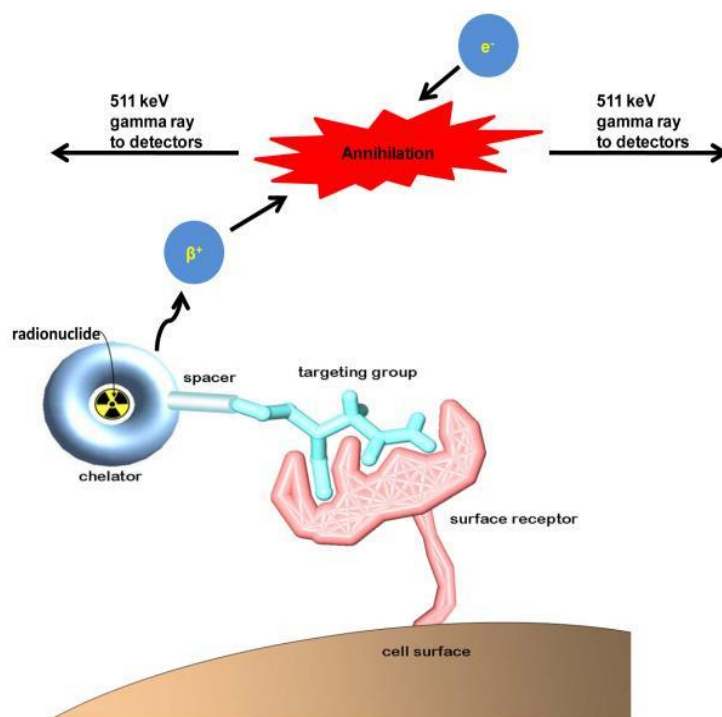
Figure 4. Principle of Positron Emission Tomography (PET) [48].

1.6   Radiometal-based radiopharmaceutical design

Functional chelators (BFCs) are used to design radiometal-based radiopharmaceuticals. They have reactive functional groups that aid its conjugation to targeting vectors such as: nucleotides, antibodies, peptides and nanoparticles. Aqueous coordination chemistry properties of each radiometal ion should be given the needed attention to harness the potential of its isotopes for medical applications. Besides, there are several key design options considered and applied across the globe [49].

1.7   Important factors for finding the optimal match between a chelator and radiometal ion

1.7.1   Thermodynamics and kinetics

Potentiometric and spectrophotometric titrations are used to determine thermodynamic stability of metal-chelate complex. pM value (-log [M]free) gives more important biological information than K_{ML}. It is a condition dependent value obtained from log K_{ML}. Both (pM and log K_{ML}) provide a number which helps the direction of metal co-ordination reactions takes under certain conditions. Unfortunately, they do not supply kinetic information such as, off-rates dissociation [1],[50, 51]. Acid dissociation experiments are important to determine the stability of metal-complex to acidic conditions. Experiments are performed at a constant PH of 2.0[21],[52, 53].

1.7.2   *In vitro* and *in vivo* stability

In vivo translation involves metal exchange competitions with mixtures that are biologically relevant. HPLC and TLC are employed to assess the quantity a radio metal trans chelates from a chelator to serum protein or enzymes. It is significant to point out that, *in vivo* gives more relevant information regarding, radiopharmaceutical stability. The higher the stability of a radiometal—chelate complex, the more a complex is removed rapidly from the kidneys and digestive systems [54-59].

1.8   Computational background

Computer models are useful regarding complexation phenomena inspection. In the absence of extensive experimental data they offer fast measurement of predictability.

1.8.1   Theoretical models

They are used in describing systems through a particular set of approximations. Depending on approximations, algorithms are then applied to atomic orbitals to calculate energies, compute frequencies and perform geometry optimizations of molecules. Quantum and non-quantum mechanical methods (use classical physics laws, such as the equation of motion [60] are employed in computational chemistry. Quantum Mechanics (QM) methods(electronic structure theories) aims at solving Schrödinger equation (1926) to study properties of molecules [61, 62]. This model consist of the following: Semi-empirical methods (employed to study large organic molecules)[63], Ab initio methods (provide accurate qualitative results as well as, quantitative estimation) for a variety of systems[64].

1.8.2   Density functional theory

To design a more effective electronic structure method, Kohn, Sham and Hohenberg proposed, density functional models[65, 66]. Electron densities are used to compute energies, instead of wave functions. The most popular among DFT methods is B3LYP. Correlation energies are calculated from electron densities using, exact exchange and gradient corrected density functional approximations [67-70].

1.8.3   Basis sets

Basis sets are used for the mathematical description of electron wave functions. Basis sets predict the shape of atomic orbitals (AOs) of the molecule using, a particular theoretical model[62] . The bigger the basis set, the better the computational output, since approximations of the orbitals gained by

imposing less restriction, on the location of electrons in space. DFT (B3LYP) method will be combined with, 6-311+G(2d,2p)[71, 72], LANL2DZ[73] and DGDZVP[74, 75] for our study.

1.8.4 Geometry optimization

Separation of nuclear and electronic degrees of freedom by Born-Oppenheimer approximation gives an idea of a chemical reaction as nuclei moves on a potential energy surface (PES). Based on transformation of one chemical species to another, easiest path from one minimum to another is along the reaction path having the lowest energy known as minimum energy path (MEP). Optimization of geometries of reactants is necessary in order to predict the lowest possible minima on the potential energy surface (PES)[62, 76].

1.8.5 Solvation studies

Self-consistent reaction field (SCRF)[77]keyword is employed to calculate the effect of solvation. This highlights the dielectric constant for the different solvents with Conductor-like Polarizable Continuum Model (CPCM)[78] and the SMD solvation model[79].

1.8.6 Computational programs

The Gauss View is a pre- and post-processor Graphical User Interface (GUI) program for Gaussian09. All molecules will be modelled, manipulated and viewed through this suite[80, 81].

1.9 Aim of the project

The main goal of this thesis is the application of quantum chemical calculations to find the optimal match between DOTA chelator and ions particularly radiometal ions applied in the field of radio-pharmaceuticals for *in vivo* radiolabeling. The loss of an ion from a chelator without reaching its target *in vivo* in the presence of competitive ions (Na^+ and K^+) could be disastrous to the human body. Employing quantum mechanical calculations we will examine the stabilities of DOTA—alkali metals complexes as well as DOTA—radiometal ions complexes. It is necessary to find out which of the radiometal ions could probably serve as the optimal match for DOTA chelator to achieve *in vivo* radiolabeling.

1.9.1   Specific objectives

A. Understanding the structure and physical properties of the chelator—radiometal ions complexes and their impact, on the overall pharmacokinetic properties of radio-pharmaceuticals.

B. Confirming aqueous co-ordination chemistry properties of radio-metal ions.

C. Examining the proposed geometry of chelator—radiometal ions complexes.

D. Comparing the stability of chelator—radiometal ions complexes as opposed to experimentally reported binding constants.

E. To propose and recommend observed chelator—radiometal ions complexes (optimal match) based on theoretical results obtained.

F. To confirm the need to carry out radio-labelling experiments involving, chelator and biologically competitive active ions based on DOTA—alkali metal ions using theoretical calculations.

1.10   Outline of this thesis

Chapter **1**, is the thesis introduction.

Chapter **2**, focus on the interactions between DOTA and alkali metal ions to compare their stabilities in gaseous and aqueous media.

Chapter **3**, investigates the interactions within DOTA—radiometal ions complexes in gaseous and aqueous media

Chapter **4**, provides a summary of the dissertation.

References

[1] Price, E. W., and Orvig, C. (2014) Matching chelators to radiometals for radiopharmaceuticals, *Chemical Society Reviews 43*, 260-290.

[2] Frost, A. E. (1956) Polyaminopolycarboxylic acids derived from polyethyleneamines.

[3] Milenic, D. E., Roselli, M., Mirzadeh, S., Pippin, C. G., Gansow, O. A., Colcher, D., Brechbiel, M. W., and Schlom, J. (2001) In vivo evaluation of bismuth-labeled monoclonal antibody comparing DTPA-derived bifunctional chelates, *Cancer Biotherapy and Radiopharmaceuticals 16*, 133-146.

[4] Roselli, M., Milenic, D. E., Brechbiel, M. W., Mirzadeh, S., Pippin, C. G., Gansow, O. A., Colcher, D., and Schlom, J. (1999) In vivo comparison of CHX-DTPA ligand isomers in athymic mice bearing carcinoma xenografts, *Cancer biotherapy & radiopharmaceuticals 14*, 209-220.

[5] Milenic, D. E., Garmestani, K., Chappell, L. L., Dadachova, E., Yordanov, A., Ma, D., Schlom, J., and Brechbiel, M. W. (2002) In vivo comparison of macrocyclic and acyclic ligands for radiolabeling of monoclonal antibodies with 177 Lu for radioimmunotherapeutic applications, *Nuclear medicine and biology 29*, 431-442.

[6] Cescato, R., Maina, T., Nock, B., Nikolopoulou, A., Charalambidis, D., Piccand, V., and Reubi, J. C. (2008) Bombesin receptor antagonists may be preferable to agonists for tumor targeting, *Journal of Nuclear Medicine 49*, 318-326.

[7] Decristoforo, C., Maina, T., Nock, B., Gabriel, M., Cordopatis, P., and Moncayo, R. (2003) 99mTc-Demotate 1: first data in tumour patients—results of a pilot/phase I study, *European journal of nuclear medicine and molecular imaging 30*, 1211-1219.

[8] Maina, T., Nock, B., Nikolopoulou, A., Sotiriou, P., Loudos, G., Maintas, D., Cordopatis, P., and Chiotellis, E. (2002) [99mTc] Demotate, a new 99mTc-based [Tyr3] octreotate analogue for the detection of somatostatin receptor-positive tumours: synthesis and preclinical results, *European journal of nuclear medicine and molecular imaging 29*, 742-753.

[9] Nock, B. A., Maina, T., Béhé, M., Nikolopoulou, A., Gotthardt, M., Schmitt, J. S., Behr, T. M., and Mäcke, H. R. (2005) CCK-2/Gastrin receptor–targeted tumor imaging with 99mTc-labeled minigastrin analogs, *Journal of Nuclear Medicine 46*, 1727-1736.

[10] Nock, B. A., Nikolopoulou, A., Galanis, A., Cordopatis, P., Waser, B., Reubi, J.-C., and Maina, T. (2005) Potent bombesin-like peptides for GRP-receptor targeting of tumors with 99mTc: a preclinical study, *Journal of medicinal chemistry 48*, 100-110.

[11] Nock, B., Nikolopoulou, A., Chiotellis, E., Loudos, G., Maintas, D., Reubi, J., and Maina, T. (2003) [99mTc] Demobesin 1, a novel potent bombesin analogue for GRP receptor-targeted tumour imaging, *European journal of nuclear medicine and molecular imaging 30*, 247-258.

[12] Buchmann, I., Henze, M., Engelbrecht, S., Eisenhut, M., Runz, A., Schäfer, M., Schilling, T., Haufe, S., Herrmann, T., and Haberkorn, U. (2007) Comparison of 68Ga-DOTATOC PET and 111In-DTPAOC (Octreoscan) SPECT in patients with neuroendocrine tumours, *European journal of nuclear medicine and molecular imaging 34*, 1617-1626.

[13] Prasanphanich, A. F., Nanda, P. K., Rold, T. L., Ma, L., Lewis, M. R., Garrison, J. C., Hoffman, T. J., Sieckman, G. L., Figueroa, S. D., and Smith, C. J. (2007) [64Cu-NOTA-8-Aoc-BBN (7-14)

NH2] targeting vector for positron-emission tomography imaging of gastrin-releasing peptide receptor-expressing tissues, *Proceedings of the National Academy of Sciences 104*, 12462-12467.

[14] Sprague, J. E., Peng, Y., Sun, X., Weisman, G. R., Wong, E. H., Achilefu, S., and Anderson, C. J. (2004) Preparation and biological evaluation of copper-64–labeled Tyr3-octreotate using a cross-bridged macrocyclic chelator, *Clinical cancer research 10*, 8674-8682.

[15] Lewis, E. A., Boyle, R. W., and Archibald, S. J. (2004) Ultrastable complexes for in vivo use: a bifunctional chelator incorporating a cross-bridged macrocycle, *Chem. Commun.*, 2212-2213.

[16] Boswell, C. A., Regino, C. A., Baidoo, K. E., Wong, K. J., Bumb, A., Xu, H., Milenic, D. E., Kelley, J. A., Lai, C. C., and Brechbiel, M. W. (2008) Synthesis of a cross-bridged cyclam derivative for peptide conjugation and 64Cu radiolabeling, *Bioconjugate chemistry 19*, 1476-1484.

[17] Notni, J., Pohle, K., and Wester, H.-J. (2012) Comparative gallium-68 labeling of TRAP-, NOTA-, and DOTA-peptides: practical consequences for the future of gallium-68-PET, *EJNMMI research 2*, 1-5.

[18] Cooper, M. S., Ma, M. T., Sunassee, K., Shaw, K. P., Williams, J. D., Paul, R. L., Donnelly, P. S., and Blower, P. J. (2012) Comparison of 64Cu-complexing bifunctional chelators for radioimmunoconjugation: labeling efficiency, specific activity, and in vitro/in vivo stability, *Bioconjugate chemistry 23*, 1029-1039.

[19] Byegård, J., Skarnemark, G., and Skålberg, M. (1999) The stability of some metal EDTA, DTPA and DOTA complexes: Application as tracers in groundwater studies, *Journal of radioanalytical and nuclear chemistry 241*, 281-290.

[20] Stimmel, J. B., and Kull, F. C. (1998) Samarium-153 and lutetium-177 chelation properties of selected macrocyclic and acyclic ligands, *Nuclear medicine and biology 25*, 117-125.

[21] Stimmel, J. B., Stockstill, M. E., and Kull Jr, F. C. (1995) Yttrium-90 Chelation Properties of Tetraazatetraacetic Acid Macrocycles, Diethylenetriaminepentaacetic Acid Analogs, and a Novel Terpyridine Acyclic Chelator, *Bioconjugate chemistry 6*, 219-225.

[22] Camera, L., Kinuya, S., Garmestani, K., Wu, C., Brechbiel, M. W., Pai, L. H., McMurry, T. J., Gansow, O. A., Pastan, I., and Paik, C. H. (1994) Evaluation of the serum stability and in vivo biodistribution of CHX-DTPA and other ligands for yttrium labeling of monoclonal antibodies, *Journal of nuclear medicine: official publication, Society of Nuclear Medicine 35*, 882-889.

[23] Harrison, A., Walker, C., Parker, D., Jankowski, K., Cox, J., Craig, A., Sansom, J., Beeley, N., Boyce, R., and Chaplin, L. (1991) The in vivo release of 90 Y from cyclic and acyclic ligand-antibody conjugates, *International journal of radiation applications and instrumentation. Part B. Nuclear medicine and biology 18*, 469-476.

[24] Hancock, R. D. (1992) Chelate ring size and metal ion selection. The basis of selectivity for metal ions in open-chain ligands and macrocycles, *Journal of chemical education 69*, 615.

[25] Stetter, H., and Frank, W. (1976) Complex Formation with Tetraazacycloalkane-N, N′, N ″, N‴-tetraacetic Acids as a Function of Ring Size, *Angewandte Chemie International Edition in English 15*, 686-686.

[26] Liu, S., and Edwards, D. S. (2001) Bifunctional chelators for therapeutic lanthanide radiopharmaceuticals, *Bioconjugate chemistry 12*, 7-34.

[27] Fani, M., Andre, J. P., and Maecke, H. R. (2008) 68Ga-PET: a powerful generator-based alternative to cyclotron-based PET radiopharmaceuticals, *Contrast media & molecular imaging 3*, 53-63.

[28] Aime, S., Cabella, C., Colombatto, S., Geninatti Crich, S., Gianolio, E., and Maggioni, F. (2002) Insights into the use of paramagnetic Gd (III) complexes in MR-molecular imaging investigations, *Journal of magnetic resonance imaging 16*, 394-406.

[29] Caravan, P. (2006) Strategies for increasing the sensitivity of gadolinium based MRI contrast agents, *Chemical Society Reviews 35*, 512-523.

[30] Heppeler, A., Froidevaux, S., Eberle, A., and Maecke, H. (2000) Receptor targeting for tumor localisation and therapy with radiopeptides, *Current medicinal chemistry 7*, 971-994.

[31] Maecke, H. R., Hofmann, M., and Haberkorn, U. (2005) 68Ga-labeled peptides in tumor imaging, *Journal of Nuclear Medicine 46*, 172S-178S.

[32] Pandya, S., Yu, J., and Parker, D. (2006) Engineering emissive europium and terbium complexes for molecular imaging and sensing, *Dalton Transactions*, 2757-2766.

[33] Reubi, J. C., Mäcke, H. R., and Krenning, E. P. (2005) Candidates for peptide receptor radiotherapy today and in the future, *Journal of Nuclear Medicine 46*, 67S-75S.

[34] Tanaka, K., and Fukase, K. (2008) PET (positron emission tomography) imaging of biomolecules using metal–DOTA complexes: a new collaborative challenge by chemists, biologists, and physicians for future diagnostics and exploration of in vivo dynamics, *Organic & biomolecular chemistry 6*, 815-828.

[35] Riesen, A., Zehnder, M., and Kaden, T. A. (1986) Metal complexes of macrocyclic ligands. Part XXIII. Synthesis, properties, and structures of mononuclear complexes with 12-and 14-membered tetraazamacrocycle-N, N′, N ″, N‴-tetraacetic Acids, *Helvetica chimica acta 69*, 2067-2073.

[36] Viola, N. A., Rarig, R. S., Ouellette, W., and Doyle, R. P. (2006) Synthesis, structure and thermal analysis of the gallium complex of 1, 4, 7, 10-tetraazacyclo-dodecane-N, N′, N ″, N‴-tetraacetic acid (DOTA), *Polyhedron 25*, 3457-3462.

[37] Benetollo, F., Bombieri, G., Calabi, L., Aime, S., and Botta, M. (2003) Structural variations across the lanthanide series of macrocyclic DOTA complexes: insights into the design of contrast agents for magnetic resonance imaging, *Inorganic chemistry 42*, 148-157.

[38] Clarke, E. T., and Martell, A. E. (1991) Potentiometric and spectrophotometric determination of the stabilities of In (III), Ga (III) and Fe (III) complexes of N, N′, N ″-tris (3, 5-dimethyl-2-hydroxybenzyl)-1, 4, 7-triazacyclononane, *Inorganica chimica acta 186*, 103-111.

[39] Liu, S., He, Z., Hsieh, W.-Y., and Fanwick, P. E. (2003) Synthesis, characterization, and X-ray crystal structure of In (DOTA-AA)(AA= p-aminoanilide): a model for 111In-labeled DOTA-biomolecule conjugates, *Inorganic chemistry 42*, 8831-8837.

[40] McEwan, A. (1997) Unsealed source therapy of painful bone metastases: an update, In *Seminars in nuclear medicine*, pp 165-182, Elsevier.

[41] Banerjee, S., Pillai, M. R. A., and Ramamoorthy, N. (2001) Evolution of Tc-99m in diagnostic radiopharmaceuticals, In *Seminars in nuclear medicine*, pp 260-277, Elsevier.

[42] Jain, D. (1999) Technetium-99m labeled myocardial perfusion imaging agents, In *Seminars in nuclear medicine*, pp 221-236, Elsevier.

[43] Jurisson, S. S., and Lydon, J. D. (1999) Potential technetium small molecule radiopharmaceuticals, *Chemical reviews 99*, 2205-2218.

[44] Liu, S. (2007) Ether and crown ether-containing cationic 99m Tc complexes useful as radiopharmaceuticals for heart imaging, *Dalton Transactions*, 1183-1193.

[45] Liu, S., and Edwards, D. S. (2002) Fundamentals of receptor-based diagnostic metalloradiopharmaceuticals, In *Contrast Agents II*, pp 259-278, Springer.

[46] Liu, S. (2004) The role of coordination chemistry in the development of target-specific radiopharmaceuticals, *Chemical Society Reviews 33*, 445-461.

[47] Reichert, D. E., Lewis, J. S., and Anderson, C. J. (1999) Metal complexes as diagnostic tools, *Coordination Chemistry Reviews 184*, 3-66.

[48] Wadas, T. J., Wong, E. H., Weisman, G. R., and Anderson, C. J. (2010) Coordinating radiometals of copper, gallium, indium, yttrium, and zirconium for PET and SPECT imaging of disease, *Chemical reviews 110*, 2858-2902.

[49] Bartholomä, M. D., Louie, A. S., Valliant, J. F., and Zubieta, J. (2010) Technetium and gallium derived radiopharmaceuticals: comparing and contrasting the chemistry of two important radiometals for the molecular imaging era, *Chemical reviews 110*, 2903-2920.

[50] Martell, A. E., and Smith, R. M. (1977) *Other organic ligands*, Vol. 3, Springer.

[51] Morfin, J.-F., and Tóth, É. (2011) Kinetics of Ga (NOTA) formation from weak Ga-citrate complexes, *Inorganic chemistry 50*, 10371-10378.

[52] Jonathan, P. (1991) Structure and solution stability of indium and gallium complexes of 1, 4, 7-triazacyclononanetriacetate and of yttrium complexes of 1, 4, 7, 10-tetraazacyclododecanetetraacetate and related ligands: kinetically stable complexes for use in imaging and radioimmunotherapy. X-Ray molecular structure of the indium and gallium complexes of 1, 4, 7-triazacyclononane-1, 4, 7-triacetic acid, *Journal of the Chemical Society, Perkin Transactions 2*, 87-99.

[53] Kubíček, V. c., Havlickova, J., Kotek, J., Tircsó, G., Hermann, P., Tóth, É., and Lukeš, I. (2010) Gallium (III) Complexes of DOTA and DOTA− Monoamide: Kinetic and Thermodynamic Studies, *Inorganic chemistry 49*, 10960-10969.

[54] Zeglis, B. M., and Lewis, J. S. (2011) A practical guide to the construction of radiometallated bioconjugates for positron emission tomography, *Dalton Transactions 40*, 6168-6195.

[55] Price, E. W., Zeglis, B. M., Cawthray, J. F., Ramogida, C. F., Ramos, N., Lewis, J. S., Adam, M. J., and Orvig, C. (2013) H4octapa-trastuzumab: versatile acyclic chelate system for 111In and 177Lu imaging and therapy, *Journal of the American Chemical Society 135*, 12707-12721.

[56] Bailey, G. A., Price, E. W., Zeglis, B. M., Ferreira, C. L., Boros, E., Lacasse, M. J., Patrick, B. O., Lewis, J. S., Adam, M. J., and Orvig, C. (2012) H2azapa: a Versatile Acyclic Multifunctional Chelator for 67Ga, 64Cu, 111In, and 177Lu, *Inorganic chemistry 51*, 12575-12589.

[57] Ferreira, C. L., Lamsa, E., Woods, M., Duan, Y., Fernando, P., Bensimon, C., Kordos, M., Guenther, K., Jurek, P., and Kiefer, G. E. (2010) Evaluation of bifunctional chelates for the development of gallium-based radiopharmaceuticals, *Bioconjugate chemistry 21*, 531-536.

[58] Ferreira, C. L., Yapp, D. T., Lamsa, E., Gleave, M., Bensimon, C., Jurek, P., and Kiefer, G. E. (2008) Evaluation of novel bifunctional chelates for the development of Cu-64-based radiopharmaceuticals, *Nuclear medicine and biology 35*, 875-882.

[59] Li, W., Ma, D., Higginbotham, C., Hoffman, T., Ketring, A., Cutler, C. S., and Jurisson, S. (2001) Development of an in vitro model for assessing the in vivo stability of lanthanide chelates, *Nuclear medicine and biology 28*, 145-154.

[60] Maeda, S., Harabuchi, Y., Ono, Y., Taketsugu, T., and Morokuma, K. (2015) Intrinsic reaction coordinate: Calculation, bifurcation, and automated search, *International Journal of Quantum Chemistry 115*, 258-269.

[61] Hehre, W. J. (2003) *A guide to molecular mechanics and quantum chemical calculations*, Wavefunction Irvine, CA.

[62] Foresman, J., and Frish, E. (1996) Exploring chemistry, *Gaussian Inc., Pittsburg, USA*.

[63] Schrödinger, E. (1926) An undulatory theory of the mechanics of atoms and molecules, *Physical Review 28*, 1049.

[64] Ghosh, S. K., and Chattaraj, P. K. (2013) *Concepts and Methods in Modern Theoretical Chemistry: Electronic Structure and Reactivity*, CRC Press.

[65] Hohenberg, P., and Kohn, W. (1964) Inhomogeneous electron gas, *Physical review 136*, B864.

[66] Kohn, W., and Sham, L. J. (1965) Self-consistent equations including exchange and correlation effects, *Physical Review 140*, A1133.

[67] Becke, A. D. (1993) Density-functional thermochemistry. III. The role of exact exchange, *The Journal of chemical physics 98*, 5648-5652.

[68] Lee, C., Yang, W., and Parr, R. G. (1988) Development of the Colle-Salvetti correlation-energy formula into a functional of the electron density, *Physical review B 37*, 785.

[69] Becke, A. D. (1988) Density-functional exchange-energy approximation with correct asymptotic behavior, *Physical review A 38*, 3098.

[70] Stephens, P., Devlin, F., Chabalowski, C., and Frisch, M. J. (1994) Ab initio calculation of vibrational absorption and circular dichroism spectra using density functional force fields, *The Journal of Physical Chemistry 98*, 11623-11627.

[71] Hehre, W. J., Ditchfield, R., and Pople, J. A. (1972) Self—consistent molecular orbital methods. XII. Further extensions of gaussian—type basis sets for use in molecular orbital studies of organic molecules, *The Journal of Chemical Physics 56*, 2257-2261.

[72] Thiel, W. (2014) Semiempirical quantum–chemical methods, *Wiley Interdisciplinary Reviews: Computational Molecular Science 4*, 145-157.

[73] Alekseev, N., Luchinin, V., and Charykov, N. (2013) Simulating the conditions for the formation of graphene and graphene nanowalls by semiempirical quantum chemical methods, *Russian Journal of Physical Chemistry A 87*, 1721-1730.

[74] Kreja, I. (2011) A literature review on computational models for laminated composite and sandwich panels, *Open Engineering 1*, 59-80.

[75] Lipinski, C. A., Lombardo, F., Dominy, B. W., and Feeney, P. J. (2012) Experimental and computational approaches to estimate solubility and permeability in drug discovery and development settings, *Advanced drug delivery reviews 64*, 4-17.

[76] Cramer, C. J. (2013) *Essentials of computational chemistry: theories and models*, John Wiley & Sons.

[77] Sadlej, J., Dobrowolski, J. C., and Rode, J. E. (2010) VCD spectroscopy as a novel probe for chirality transfer in molecular interactions, *Chemical Society Reviews 39*, 1478-1488.

[78] Rega, N., Cossi, M., and Barone, V. (1999) Improving performance of polarizable continuum model for study of large molecules in solution, *Journal of computational chemistry 20*, 1186-1198.

[79] Marenich, A. V., Cramer, C. J., and Truhlar, D. G. (2009) Universal solvation model based on solute electron density and on a continuum model of the solvent defined by the bulk dielectric constant and atomic surface tensions, *The Journal of Physical Chemistry B 113*, 6378-6396.

[80] Dennington, R., Keith, T., and Millam, J. (2009) Semichem Inc, *Shawnee Mission KS, GaussView, Version 5*.

[81] Frisch, M., Trucks, G., Schlegel, H., Scuseria, G., Robb, M., Cheeseman, J., Scalmani, G., Barone, V., Mennucci, B., and Petersson, G. (2009) gaussian 09, Gaussian, *Inc., Wallingford, CT 4*.

CHAPTER 2

DFT Study of the Interactions between DOTA Chelator and Competitive Alkali Metal Ions

E. Frimpong, A. A. Skelton[*], B. Honarparvar[*]

School of Pharmacy and Pharmacology, University of KwaZulu-Natal, Durban 4001, South Africa

Corresponding authors: Honarparvar@ukzn.ac.za (B. Honarparvar), Skelton@ukzn.ac.za (A.A Skelton) School of Pharmacy and Pharmacology, University of KwaZulu-Natal, Durban 4001, South Africa. Tel.: +27 31 26084, +27 31 2608520

Abstract

1, 4, 7, 10-tetraazacyclododecane-1, 4, 7, 10-tetracetic acid (DOTA) is an important chelator for radiolabeling of pharmaceuticals. The ability of alkali metals, found in the body, to complex with DOTA and compete with radio metals can alter the radiolabeling process. Non-covalent interactions between DOTA complexed with alkali metals, Li^+, Na^+, K^+ and Rb^+, were investigated with density functional theory using B3LYP and ωB97XD functionals with 6-311+G (2d, 2p) basis set for Li^+, Na^+ and K^+ and Def2-TZVPD for Rb^+. Conformational possibilities were explored in terms of a different number of carboxylic pendant arms of DOTA in in close proximity to the ions. It is found that the case in which four arms of DOTA are interacting with ions is more stable in comparison to other conformations.

The core objective of this study is to explore the electronic structure properties upon complexation of alkali metals, Li^+ Na^+, K^+ and Rb^+, with DOTA chelator. Interaction energies, relaxation energies, entropies, Gibbs free energies and enthalpies show that the stability of DOTA, complexed with alkali metals decreases down the group of the periodic table. Implicit water solvation affects the complexation of DOTA—ions leading to decreases in the stability of the complexes. NBO analysis through the natural population charges and the second order perturbation theory reveals charge transfer between DOTA and alkali metals. Conceptual DFT-based properties such as HOMO/LUMO energies, $\Delta E_{HOMO-LUMO}$ and chemical hardness and softness reveal the decrease in chemical stability of

DOTA—alkali metal complexes down the alkali metal series. This study serves as a guide to researchers in the field of organometallic chelators, particularly, radio-pharmaceuticals in finding the efficient optimal match between chelators and different metal ions.

Keywords: Density functional theory (DFT); 1, 4, 7, 10-tetraazacyclododecane-1, 4, 7, 10-tetracetic acid (DOTA); Natural bond orbital (NBO).

2.1   Introduction

Organometallic chelators can be potentially used for radio-metal-based pharmaceuticals [1, 2] where the radiolabeled chelator complexes are used as biological vehicles for imaging in the field of medicine[3, 4]. The bifunctional chelator, which is covalently bound to a lead compound forms a stable chelator—ion complex to deliver an isotope, as a labelling agent, towards a specific *in vivo* target [5]. The 1, 4, 7, 10-tetra acetic acid, DOTA, is a twelve-membered tetra aza macro cycle (**Figure 1**), which contains four pendant carboxylate arms connected to cyclen amines.
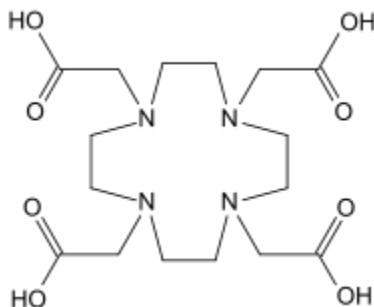
Figure 1. The structure of 1, 4, 7, 10-tetraazacyclododecane-1, 4, 7, 10-tetraacetic acid (DOTA)

Several pharmacokinetic and structural studies in the field of coordination chemistry have been performed on radio metals complexes, with DOTA derivatives, to gain deep insight into metal based pharmaceutics [6-11] . To the best of our knowledge, despite comprehensive efforts made on radio-metals complexed with DOTA chelator, there has been less attention on finding the optimal match of DOTA chelator with alkali metal ions, found in the body, which can act as competitors to radio metals. In the light of this fact, the present study reports electronic structure calculations using density functional theory (B3LYP functional) with 6-311+G (2d, 2p) basis set for Li$^+$, Na$^+$ and K$^+$ and Def2-TZVPD for Rb$^+$ to provide insight into the essential factors affecting the chelating ability of DOTA with alkali

metals. This can be expanded into exploiting the possible impacts of these competitive ions on the radiolabeling yield of this chelator, which is useful in predicting the efficiency of the complexation of DOTA with radio metals, in the presence of other ions, *in vivo*. To gain an in-depth insight into the complexation of DOTA with alkali metals, the interaction of DOTA—alkali metal complexes and other thermodynamic properties such as relaxation energies, entropy, enthalpy, Gibbs free energy, and the interatomic distances within DOTA-alkali metal complexes will be reported. NBO analysis and DFT-based reactivity descriptors, the electron affinity (EA), ionization potential (IP), chemical softness (*S*) and hardness (η) are also discussed.

2.2   Computational details

The B3LYP density functional is widely used for *in silico* electronic structure analysis because it could give reasonable energies, molecular structures and vibrational frequencies [12, 13]. B3LYP density functional [14-16] with 6-311G+ (2d, 2p) basis set using Gaussian 09 program[17] were employed in the present study for DOTA chelator and the selected Li^+, Na^+ and K^+ ions. The Def2-TPVZ basis set was used for Rb^+, which is described by the effective core potential (ECP) of Wadt and Hay [18-23]. Full geometry optimizations of all the species were carried out. BSSE calculations are performed to test the effect of a finite basis set. Interaction energy (E_{int}) is defined as:

$$E_{int} = E_{DOTA-ion\ complex} - E_{DOTA} - E_{ion} \qquad (1)$$

The ion described in the equation could be Li^+, Na^+, K^+ and Rb^+ Relaxation energies were calculated by subtracting the complexation energy values (unrelaxed) from the interaction energies (relaxed). After the geometry optimization of the DOTA—cation complexes, the cation was removed from DOTA and a single point energy of DOTA in the same configuration was performed. Secondly, a further geometry optimization of the DOTA was performed to enable DOTA to relax. The differences in energies between the two aforementioned cases is called the relaxation energy, which provides a measure of how the ion affects the conformation of the DOTA. Intermolecular short-range distances ≤3.5Å between the ions and the hetero atoms are recorded. To consider the long-range and dispersion contribution in the E_{int} values of DOTA—ion further calculations were performed with the ωB97XD density functional.[24]

Natural bond orbital (NBO) analysis was performed using NBO program implemented in Gaussian 09 program package. NBO analysis could highlight the role of intermolecular orbital interaction in the complexes, particularly the charge transfer between DOTA and ions by considering all possible interactions between filled donor and empty acceptor NBOs, and estimating their energetic significance with second-order perturbation theory. The second-order Fock matrix was employed to evaluate the donor-acceptor interactions in the NBO basis[25]. Second perturbation theory confirms whether there is an electron donation from one atom to another. This electron donation results in the stabilization of energy, E^2:

$$E^2 = \frac{q_i F(i,j)^2}{\varepsilon_j - \varepsilon_i} \tag{2}$$

Here q_i is the orbital occupancy, while ε_i, ε_j and $F_{i,j}$ are the diagonal and the off-diagonal NBO Fock matrix elements, respectively.

Atoms in each complex were categorized in terms of their short-range distance with ions ($\leq$3.5Å range), after the geometry optimizations. The DFT based reactivity descriptors calculations were preformed using the following equations [26-29]:

Chemical hardness is defined as:

$$\eta = \frac{IP - EA}{2} \tag{3}$$

and softness,

$$S = \frac{1}{2\eta} \tag{4}$$

Ionization potential (IP) was obtained by using energy differences, between radical cation, Ec and the respective neutral molecule, $IP = E_c - E_n$. Electron affinity (EA) was calculated by the energy differences between a radical anion, Ea and the respective neutral molecule, $EA = E_a - E_n$. The term "neutral" is the standard charge state, for instance, the ions have +1 charge and cationic and anionic species have +2 and 0 charges, respectively. Thermodynamic properties (enthalpy, free energy and entropy with different translational, vibrational and rotational contributions) are calculated by normal mode analysis [30] The Polarizable Continuum Model (PCM), using the integral equation-formalism polarizable continuum model (IEF-PCM), was used to evaluate the solvent effect on the NOTA complexation with alkali metals[31] [31] Finally, the eigenvalues of the highest occupied molecular orbital

(HOMO) and the lowest unoccupied molecular orbital (LUMO) of all the DOTA—ion complexes were calculated at the same level of theory.

2.3 Results and Discussions

For lucid data interpretation and assessing how various functional groups in pendant arms contributed to the geometries and electronic structure properties of the DOTA—alkali metal ion complexes, classification of various atomic groups were considered in terms of their close contact with an ion. (**Figure 2**).

2.3.1 Energetics of conformational analysis

Four carboxylic pendant arms in DOTA provide different conformational possibilities, where a different number of arms are coordinating towards the ions. The crystal structure of DOTA— Sc^{3+2}, where all four pendent arms and nitrogen atoms are in close proximity with Sc^{3+}, was considered as a starting structure for DOTA—alkali metal ion complexes. To do this, Sc^{3+} was replaced by Li^+, Na^+, K^+ and Rb^+ and geometry optimizations were performed, which are shown in **Figures 2a** and **2b**. It can be noticed that in the case of Na^+, K^+ and Rb^+, all four pendant arms remain in close proximity to the ions, whereas in the case of Li^+, two of the pendant arms remained in close proximity (α) and two pendant arms moved farther away from the ion (β).

To evaluate different conformational possibilities, carboxylic pendant arms were systematically moved farther away from the ions and geometry optimizations were performed. In both vacuum and water media, it was observed that for all ions the conformation with four arms interacting with ions had the lowest energy in comparison to other possibilities; however, for Li^+ the three arm conformation had a similar energy to that of the crystal structure (**Figure 2c**). This observation can be attributed to the fact that within optimization the four arm conformation was converted to two arms.
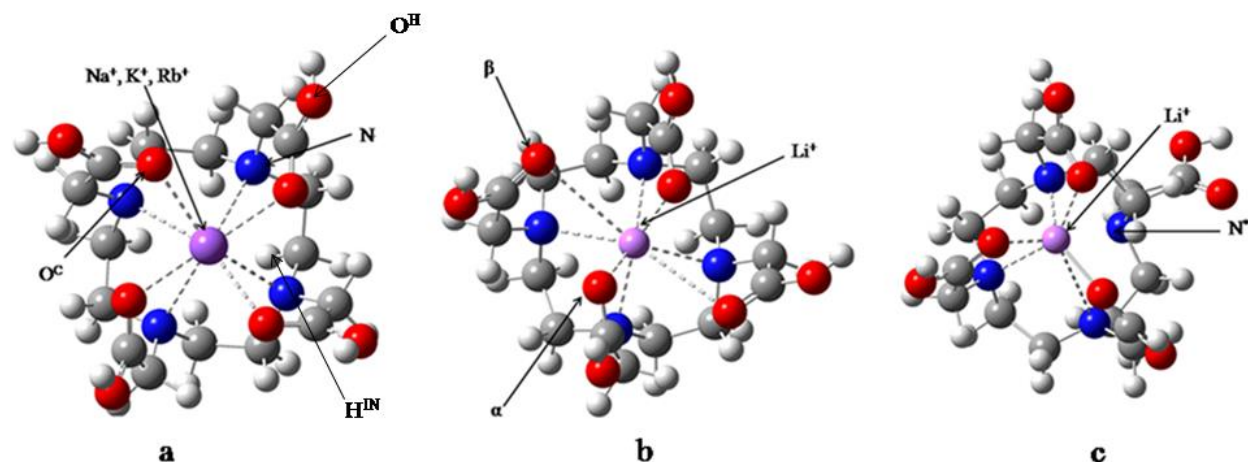
Figure 2. Optimized structures of DOTA—ion complexes: DOTA—Na$^+$, DOTA—Li$^+$, DOTA—K$^+$ and DOTA—Rb$^+$. Intermolecular distances between heteroatoms and ions in close proximity are represented by dotted ions. DOTA—Li$^+$, DOTA—Na$^+$, DOTA—K$^+$ and DOTA—Rb$^+$ have 4N and 4O in close proximity. Carbonyl oxygen in close contact with an ion (O^C). Nitrogen and carbonyl oxygen in close contact with an ion (N). Nitrogen and carbonyl oxygen not in close contact with an ion (N*).

The four arm conformation, for all ions, was considered as the reference to calculate relative energies ($\Delta E_{relative}$) for different DOTA—ion complexes (**Table 1**).

Table 1. Relative energies for different DOTA— ion complexes. All energies are in kcal/mol.

Complexes	$\Delta E_{relative}$ Crystal structure (kcal/mol)	$\Delta E_{relative}$ 2 Arms (kcal/mol)	$\Delta E_{relative}$ 3 Arms (kcal/mol)
DOTA—Li$^+$	0 (0)	6.83 (1.64)	0.22 (1.70)
DOTA—Na$^+$	0 (0)	14.45 (6.08)	8.23 (6.30)
DOTA—K$^+$	0 (0)	13.32 (7.10)	7.86 (6.04)
DOTA—Rb$^+$	0 (0)	11.28 (5.63)	6.36 (4.58)

Parentheses show values for water medium.

According **Table 1**, for Li$^+$, K$^+$, and Rb$^+$ ions there is a systematic increase in complex stability with increasing the number of pendant arms in close proximity to the ions. For Li$^+$, however, the 3 arm configuration is close in energy to the crystal structure and this is probably due to the smaller size of Li$^+$ than the other ions and the decrease in intrinsic coordination number of Li$^+$. Overall, water medium decreased the difference in relative energies of the different conformations, which would allow the complexes to span more conformational possibilities.

2.3.2 Interaction and relaxation energies

To understand the conformational preferences of the DOTA―alkali metal ion complexes and quantify the interactions within each complex, the interaction energies (E_{int}) of the DOTA―alkali metal ion complexes using both B3LYP and ωB97XD density functionals, relaxation energies (E_{relax}) and basis set superposition errors (BSSE) for the complexes are discussed in this section. The E_{int} values of the complexes in vacuum and water media, relaxation energies and BSSE energy values of the DOTA―alkali metal ion complexes are listed in **Table 2.**

Table 2. The interaction, relaxation and counterpoise corrected energies of the DOTA―alkali metal ion complexes in vacuum and solvent obtained by B3LY P/6-311G+(2d,2p) and Def2-TPVZ basis set for Rb^+. To consider the effect of dispersion on E_{int} the data for ωB97XD is also reported.

DOTA―ion complexes	E_{int} (kcal mol^{-1})		E_{relax} (kcal mol^{-1})	E_{BSSE} (kcal mol^{-1})
	B3LYP	ωB97XD		
DOTA―Li$^+$	-104.63 (-13.96)	-106.74	29.97	1.15
DOTA―Na$^+$	-85.80 (-14.92)	-86.86	27.87	2.06
DOTA―K$^+$	-60.70 (-10.96)	-61.00	25.15	1.08
DOTA―Rb$^+$	-49.20 (-5.33)	-51.70	24.93	0.57

E_{int}: Interaction energy; E_{relax}: Relaxation energy; E_{BSSE} : Basis sets superposition error. Parentheses show values for water medium.

The most negative interaction energy, which indicates the strongest intermolecular chelator―ion interaction, was found for DOTA―Li$^+$ complex. In general, the E_{int} values for DOTA complexation with alkali metal ions follow a decreasing order: DOTA―Li$^+$ > DOTA―Na$^+$ > DOTA―K$^+$> DOTA―Rb$^+$. This observation confirms stronger intermolecular interaction, which leads to greater complex stability, for DOTA―Li$^+$ complex with smaller atomic radii of ion than the others. This observation is consistent with the increased values of the distances between the hetero-atoms and the ions in the complexes, down the series (see section 3.5). To consider the long-range and dispersion contribution in the E_{int} values of DOTA―ion further calculations were performed with the ωB97XD density functional. It can be noticed that there are insignificant differences between ωB97XD and B3LYP functionals; however, the obtained E_{int} values of ωB97XD are slightly more negative than that of B3LYP.

Relaxation energies (E_{relax}) are derived by subtracting the complexation energies (unrelaxed) from the interaction energy value (relaxed) and provides a measure of how an ion can induce a specific conformation on the DOTA chelator. The E_{relax} values decrease down the periodic table for all complexes implies the larger the intermolecular interaction in DOTA―alkali metal complexes, the more the ion can induce a specific conformation that would be different from its preferred conformation.

It is notable that the E_{relax} values decreased with the increase in the atomic radii of the ions upon complexation with DOTA; that is, the inducing effects of the ions on the conformation of the complexes decreases with the strength of the DOTA―ion interactions. The BSSE energies obtained for the various complexes were ≤ 2 kcal mol^{-1}, which confirms the suitability and effectiveness of the size of the basis sets for the considered complexes.

As for the solvent effect, it can be inferred that in the presence of water, the interaction energies of all DOTA―ion complexes are significantly less negative, and, therefore, less stable than in vacuum. In fact, the trend in the interaction energies is altered by water solvation; that is, the E_{int} value of Na$^+$ is greater than that of Li$^+$ and might be due to the presence of four pendant carboxylic arms interacting with Na$^+$ compared to two for Li$^+$ (**Figure 2**). Indeed, water interferes with the interaction of DOTA with the ions, and therefore reduces the chelation possibility.

2.3.3 Thermodynamic properties

For further understanding of the favorability of DOTA―ion complexation, the enthalpies, free energies, entropy and its individual contributions (translational, rotational, and vibrational) of the alkali metals complexed with DOTA are reported in **Table 3**.

Table 3. Thermodynamic properties of the alkali metal complexed with DOTA obtained by B3LYP/6-311G+(2d,2p) and Def2-TPVZ basis set for Rb^+.

Complexes	ΔH (kcal mol^{-1})	ΔG (kcal mol^{-1})	ΔS (cal mol^{-1} K^{-1})	ΔS_{Rot} cal mol^{-1} K^{-1})	ΔS_{Trans} (cal mol^{-1} K^{-1})	ΔS_{Vib} cal mol^{-1} K^{-1})
DOTA—Li$^+$	-103.33	-94.72	-28.87	-0.06	-31.75	2.94
	[-11.96]	[-3.27]	[-29.14]	[-0.13]	[-31.75]	[2.74]
DOTA—Na$^+$	-85.07	-75.78	-31.18	0.06	-35.17	3.93
	[-13.73]	[-4.82]	[-29.88]	[-0.04]	[-35.17]	[5.32]
DOTA—K$^+$	-60.16	-51.93	-27.62	0.38	-36.63	8.64
	[-10.37]	[-2.75]	[-25.58]	[0.30]	[-36.63]	[10.76]
DOTA—Rb$^+$	-48.91	-41.83	-23.76	0.58	-38.66	14.32
	[-4.67]	[2.51]	[-24.09]	[0.50]	[-38.66]	[14.09]

Brackets ([]) indicate results obtained in solvent medium.

The ΔH values recorded for all complexes are slightly less negative than its interaction energy, E_{int} (**Tables 2** and **3**). The ΔH and ΔG values for the complexes in all cases become less negative down the alkali metal series which implies the decreases in the strength of DOTA—ion complexation down the group. In the presence of the solvent, the enthalpy and Gibbs free energies showed more negative values compared to vacuum, which reveals the less interactions between DOTA and the ions in water medium. The ΔS values for all complexes become less negative from Na$^+$ to Rb$^+$; this decrease in entropy of the complex, acts against the stability of the DOTA—alkali metal complexes ($\Delta G=\Delta H$-TΔS). In the case of Li$^+$, the ΔS is less negative than Na$^+$ and does not follow the aforementioned trend. This can be attributed to the interaction of only two carboxylic pendant arms for Li$^+$, which provides a greater entropy within the complex.

Due to the negative ΔS values for all ions, the ΔG values are all less negative than their corresponding ΔH values. The rotational and vibrational contributions to entropy (ΔS_{rot} and ΔS_{vib}) become more positive down the series. The various complexes show negative translational contributions to the entropy (ΔS_{trans}) because each complex is made up of two components, namely an ion and ligand. The ΔS_{trans} values for all the complexes become more negative down the group, and this could be attributed to the increase in absolute translation entropies (**Table S1**) for the free cations. The entropy values in solvent medium increase down the group and show a similar trend to the corresponding values in the vacuum.

Taken together, the reported thermochemical parameters show that the complexation of DOTA with alkali metal ions in water is less favorable and less stable than vacuum. The formation of DOTA—Rb$^+$ complex appears to be significantly less preferable than other complexes.

2.3.4 Interatomic distances

The calculated interatomic distances in vacuum and water media are shown in **Table 4** to compare inter-molecular distances between ions and hetero-atoms in both phases.

Table 4. The average interatomic distances (Å) between ions and N, O atoms of DOTA ($\leq$3.5 Å) obtained by the DFT/B3LYP method with 6-311 G+ (2d, 2p) as basis set and Def2-TPVZ for Rb$^+$.

Complexes	O^C—ion distances (Å)	N—ion distances (Å)
DOTA—Li$^+$	2.07[2.14]$^\alpha$ (2) 3.23[3.36]$^\beta$ (2)	2.41[2.40] (4)
DOTA—Na$^+$	2.49[2.55] (4)	2.69[2.66] (4)
DOTA—K$^+$	2.77[2.82] (4)	3.03[2.99] (4)
DOTA—Rb$^+$	2.93[2.99] (4)	3.26[3.21] (4)

Brackets ([]) indicate the values obtained in the aqueous medium. Parentheses ( ) indicate number (sum) in each sub-category.

According to **Table 4**, for Li$^+$, two different values for O^C—ions distances are observed for α and β (**Figure 2**). The shorter intermolecular heteroatom—ion distances within complexes, correspond to the complexes with the more negative E$_{int}$ values (**Table 1**) in both vacuum and aqueous media. It is worth noting that, the distances between nitrogen atoms and ions are larger than that of oxygen atoms; this indicates that the strength of interaction is greater between oxygen atoms of DOTA and ions than nitrogen atoms. The average interatomic distances (Å) between ions and N, O atoms of DOTA within 3-arm conformations of DOTA—alkali metal complexes are reported in **Table S2**. In general, the O^C—ion and N—ion distances are shorter for the 3-arm conformation than 4-arm, crystal structure; this is due to a lower number of heteroatoms that are in close proximity, which leads to less competition for interacting with ions.

2.3.5 Natural bond orbital (NBO) analysis

The charge transfer within the chelator-ion complexes is one of the essential factors for the interaction of DOTA with alkali metals. Charge transfer can be investigated using natural bond orbital (NBO) analysis [32] by monitoring the atom charges, change of atom charges upon complexation, and second order perturbation theory.

2.3.5.1 Natural atomic charge analysis

Natural atomic charge (NAC) analysis can be used to monitor the atomic charge transfer, which may occur upon complexation [25, 32] . **Table 5** lists the NAC values of atoms within defined sub-categories (**Figure 2**) in each DOTA—ion complex

Table 5. Natural atomic charges (NAC) of classified atoms obtained by B3LYP/6-311+G(2d,2p) and Rb^+(Def2-TPVZ). The reported values are the average of all natural atomic charges in the classified group.

Atoms	Free DOTA	DOTA—Li$^+$		DOTA—Na$^+$	DOTA—K$^+$	DOTA—Rb$^+$
Li$^+$, Na$^+$, K$^+$, Rb$^+$	—	0.461[0.470]		0.532[0.521]	0.621[0.621]	0.600[0.590]
O^C	-0.640 [-0.665] (4)	-0.607 [-0.616]$^\alpha$ (2)	-0.594 [-0.614]$^\beta$ (2)	-0.604 [-0.614] (4)	-0.600 [-0.613] (4)	-0.597 [-0.609] (4)
N	-0.567 [-0.574] (4)	-0.578 [-0.579] (4)		-0.575 [-0.576] (4)	-0.566 [-0.568] (4)	-0.563 [-0.564] (4)
H^{IN}	0.186 [0.193] (16)	0.200 [0.204] (16)		0.197 [0.200] (16)	0.196 [0.199] (16)	0.195 [0.197] (16)

Brackets ([]) indicate results obtained in solvent media. Parentheses ( ) indicate number (sum) in each sub-category.

According to the reported NAC data in **Table 5,** it was realized that Li$^+$ with a deficit of 1e$^-$ is less electron deficient (0.461 e$^-$) upon complexation with DOTA. This effect was less evident, down the series; namely, Na$^+$ became less deficient (0.532 e$^-$) followed by K$^+$ (0.621 e$^-$) and Rb (0.600 e$^-$). Natural atomic charges of ions, within 3-arm conformations of DOTA—alkali metal complexes are less negative (**Table S3**) than within the 4-arm, crystal structure; this is due to less intermolecular interactions in the former case (**Table 1**).

For the both N and O^C atoms, within the complexes, NAC values became less negative down the alkali metal series; this could be due to the possibility of charge transfer from DOTA to the ions which depends on the size of ions. For free DOTA, the NAC values for O^C are more negative than those in the complexes and this is attributed to the lack of charge transfer from O^C to the ions, which leads to an accumulation of charge on these atoms. In the case of N atoms, the NAC values for the free DOTA are less negative than Li$^+$ and Na$^+$ while more negative than K$^+$ and Rb$^+$ complexes. It can be infered that the influence of the ion on the NAC value of N is smaller than the influence of the ion on the O^C NAC value because the N—ion distances are smaller than the O^C—ion distances (**Table 4**).

Lower average NAC values of H^{IN} for free DOTA compared to the complexes revealed that H^{IN} atoms serve as an electron resource for charge transfer from DOTA to the ions within the complexes; this

effect decreases down the alkali metal series. Overall, it seems that the non-covalent interactions within DOTA—ion complexes led to electron exchange from DOTA to the ions.

2.3.5.2 Second perturbation stabilization energies

In this section, the possible charge transfer within DOTA and between DOTA and the alkali metal ions, using second order perturbation, is discussed. Second-order perturbation theory analysis for all the complexes is presented in the **Table 6,** which shows the average stabilization E^2 values. The larger the E^2 value, the greater the charge transfer between electron donors and electron acceptors[33].

Table 6. The second-order perturbation energies, $E^{(2)}$ (kcal/mol), corresponding to significant donor $\rightarrow$ acceptor charge transfers within DOTA—alkali metal complexes obtained by B3LYP/6-311+G(d,p) level of theory and Def2-TPVZ basis set for Rb^{+}.

Complexes	Donor	Acceptor	E^2(kcal/mol)
Within DOTA			
DOTA—Li^{+}	LP (O[H])	σ* (C-O)	52.33[α],45.13[β]
DOTA—Na^{+}	LP (O[H])	σ* (C-O)	49.10
DOTA—K^{+}	LP (O[H])	σ* (C-O)	48.60
DOTA—Rb^{+}	LP (O[H])	σ* (C-O)	45.70
DOTA	LP (O[H])	σ* (C-O)	51.26
From DOTA to ions			
DOTA—Li^{+}	LP (O[C])	LP* (Li^{+})	15.4[α], 6.5[β]
DOTA—Na^{+}	LP (O[C])	LP* (Na^{+})	9.41
DOTA—K^{+}	LP (O[C])	LP* (K^{+})	8.10
DOTA—Rb^{+}	LP (O[C])	LP* (Rb^{+})	9.33

$E^{(2)}$ is the energy of stablization . LP is lone pair σ* (anti-bonding orbitals);C=O :carbonyl bond.

Table 6 shows selected values obtained by second-order pertubation theory within NBO analysis; this approach indicates whether there is electron donation from one atom to another resulting in stablization energy of a system. The donor-acceptor orbitals, within DOTA and from DOTA to the ions, were considered.

In all cases, the largest stabilization is given by charge transfer from LP on O[H] to the O[C] (bond). In the case of Li^{+}, there are two separate values for α and β, where the α value with a closer proximity to the ion shows greater charge transfer (**Table 4**). There is significant charge transfer from the LP of the O[C] to LP* of the ions. Likewise, there are two separate values for α and β for DOTA to Li^{+} charge transfer. In comparison to O[C], there is no significant charge transfer from nitrogen atoms to the ions

and this could be attributed to the longer N—ion interactomic distances than that of O^C—ion (**Table 4**).

The possibility of charge transfer, within DOTA and from DOTA to ions, which leads to stabilization energy is more evident down the alkali metal series. A schematic representation of charge transfer that occurs from the DOTA molecule to the ions is represented in **Figure 4**, where arrows show the direction of charge transfer.
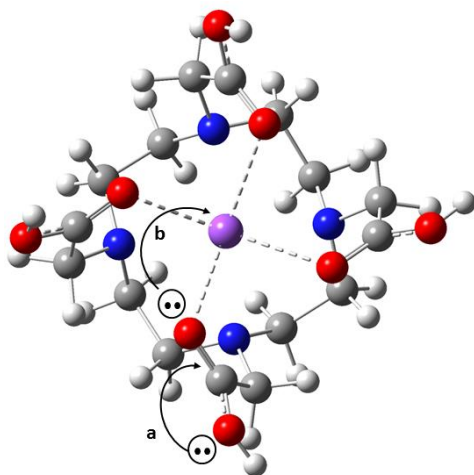
Figure 4. A presentation of the charge transfer for DOTA—ion complexes shown in NBO analysis using second perturbation theory. **a** and **b** demonstrate the direction of charge transfer. **a**. LP (O^H) → σ* (C-O) **b**. LP (O^C) → LP* (Ion).

2.3.6   Analysis of frontier molecular orbitals

The energy eigenvalues of the frontier molecular orbitals, E_{HOMO} and E_{LUMO}, are the commonly-used quantum chemical quantities that determine the chemical stability[34, 35]. The $\Delta E_{LUMO\text{-}HOMO}$ gap is a quantum chemical stability parameter,[36] the higher its value, the more stable the chemical system[37]. These parameters can also indicate how the presence of ion can affect the stability of the systems. To assess the stability of complexation, the E_{HOMO} and E_{LUMO} energy eigenstate of the DOTA—ion complexes, and individual components in the complexes, are reported in **Table 6**.

Table 7. The energy eigenvalues of the frontier molecular orbitals (E_{HOMO}, E_{LUMO}) for the selected alkali metal ions and DOTA—alkali metal ion complexes obtained by B3LYP/6-311G+(2d,2p) and Def2-TPVZ for Rb^+.

Complexes/ions	E_{HOMO} /eV	E_{LUMO} /eV	$\Delta E_{LUMO\text{-}HOMO}$ /eV
Li^+	-63.92	-6.95	56.97
Na^+	-39.16	-7.10	32.05
K^+	-26.52	-5.94	20.59
Rb^+	-22.88	-5.53	17.34
DOTA	-6.06	-0.91	5.15
DOTA—Li^+	-9.60	-3.42	6.18
DOTA—Na^+	-9.45	-3.38	6.07
DOTA—K^+	-9.44	-3.32	6.12
DOTA—Rb^+	-9.39	-3.31	6.08

The E_{HOMO} energy eigenvalue of the free alkali metal ions become less negative down the series and it can be noticed that the larger the atomic radius of an ion, the smaller its $\Delta E_{LUMO\text{-}HOMO}$ energy gap. It can be observed that the presence of the ion, in the DOTA—ion complexes, has a significant influence on the E_{HOMO} and $\Delta E_{LUMO\text{-}HOMO}$ of the complexes. The more positive E_{HOMO} and greater $\Delta E_{LUMO\text{-}HOMO}$ reflect the increase in complex stabilities in the presence of ions and this effect is decreased down the group.

2.3.7 Conceptual DFT-based properties upon complexation

Density functional theory method can be applied to calculate specific electronic structure properties such as hardness and softness [38], which are related to chelator—ion complexation. Ionization potential (IP) and electron affinity (EA) indicate the tendency of an atom or molecule to donate and attract electrons, respectively. Chemical hardness (η) is a significant parameter that describes the resistance in disruption in electron charge distribution, and correlates with the stability and reactivity of the DOTA—ion complexes [39, 40].

Table 8. DFT-based quantities for DOTA chelator complexed with alkali metals (Li$^+$, Na$^+$, K$^+$ and Rb$^+$) obtained by B3LYP/6-311G+(2d,2p) and Def2-TPVZ for Rb$^+$.

System	EA (eV)	IP (eV)	η (eV)	S (eV)
Li$^+$	-5.62	76.04	40.83	0.01
Na$^+$	-5.42	47.62	26.52	0.02
K$^+$	-4.50	31.69	18.10	0.03
Rb$^+$	-4.30	27.92	16.11	0.03
DOTA	0.34	7.19	3.42	0.1459
DOTA—Li$^+$	-2.32	11.01	6.66	0.0750
DOTA—Na$^+$	-2.29	10.87	6.58	0.0760
DOTA—K$^+$	-2.27	10.85	6.56	0.0763
DOTA—Rb$^+$	-2.08	10.79	6.43	0.0777

The EA value, for the free alkali metals, becomes less negative while IP becomes less positive; this manifests itself in a decreasing chemical hardness as the atomic radius increases and electron density is more disperse around the nucleus. A comparison of free DOTA with the complexes revealed that the presence of the ions leads to an increase in chemical hardness and decrease in softness, an increase in stability upon DOTA—ion complexation. It is notable that the smaller the ion, the greater the hardness, this observation being consistent with our earlier observed trend in both interaction energies and thermochemical properties (**Tables 2** and **3**). It is significant to point out that there is a reasonable correlation between hardness (**Tables 8**) and the observed $\Delta E_{LUMO\text{-}HOMO}$ values (**Tables 7**) obtained for the DOTA—Na$^+$, K$^+$, Rb$^+$ complexes; that is, the larger the energy gap of a molecule, the higher its hardness value; this is consistent with the literature [34, 35].

2.3.8   Implication of results for radio-pharmaceuticals

The stability of radio-chelator complex affects radiolabeling efficiency *in vivo*[5] which is a key factor to reduce tissue damage upon radiation. For instance, premature release of $^{90}Y^{3+}$ from a chelator in vivo could cause myelo-suppression as a result of irradiation from the proximate bone marrow[41]. In this context, the presence of competitive alkali metals in the body could affect the radiolabelling yield of DOTA where there is displacement of radio metals by alkali metals that are abundant in the body. The calculation of interaction energy is an essential approach to tackle the strength of chelation and, therefore, the competitive ability of the alkali metal with radio metals and other possible ions. In this study, the E_{int} values for DOTA complexation with alkali metal ions follow a decreasing order from Li$^+$ to Rb$^+$. In water medium, however, the E_{int} value of Na$^+$ is greater than that of Li$^+$.

The total concentrations of alkali metals in our body are as follows: Li^+ $(3.1\times10^{-6}$ mg/kg), Na^+ $(2.5\times10^{-3}$ mg/kg), K^+ $(1.5\times10^{-3}$ mg/kg) and Rb^+ $(4.6\times10^{-6}$ mg/kg $)^{42}$ and this provides further insight into the possibility of ion competition. Since Na^+ ions are the most abundant and, in solution, the strongest binders to DOTA, these ions are most likely to destabilize DOTA—radio metal complexes which we are investigating in our ongoing project.

2.4   Conclusions

The non-covalent interactions between hetero-atoms of DOTA and the selected alkali metal ions, Li^+, Na^+, K^+ and Rb^+, were investigated using density functional theory (DFT). Three different conformations of DOTA—ion complexes, namely 2-arm, 3-arm and 4-arm crystal structure, were considered; it was found that the 4-arm, which was derived from the crystal structure of DOTA—Sc^{3+} [2] had the lowest energy for all complexes. The interaction energies and other electronic structure properties of DOTA—ion complexes were investigated. The observed charge transfer, from the lone pairs of O^H to the carbonyl antibonding orbitals and also the lone pairs of O^C to the lone pair (LP*) of the ions, plays a crucial role to the DOTA chelation.

The outcome of this study is that the interaction energies, bond distances, natural atomic charge, conceptual DFT-based properties including chemical hardness and softness exhibited a considerable intermolecular interaction between DOTA and alkali metal ions.

It is concluded that the stability of DOTA–alkali metal complexes decreases down the periodic table. Consequently, the presence of alkali metal ions, particularly Na^+, which is the most abundant ions in biological systems, can compete with radiometals for complexation with DOTA and affect the imaging. Understanding the competitive non-covalent interactions of DOTA with alkali metals will provide important information for the optimal match of DOTA with radio metals which is currently under investigation.

References

[1] Kerdjoudj, R., Pniok, M., Alliot, C., Kubíček, V., Havlíčková, J., Rösch, F., Hermann, P., and Huclier-Markai, S. (2016) Scandium (iii) complexes of monophosphorus acid DOTA analogues: a thermodynamic and radiolabelling study with 44 Sc from cyclotron and from a 44 Ti/44 Sc generator, *Dalton Transactions 45*, 1398-1409.

[2] Pniok, M., Kubíček, V., Havlíčková, J., Kotek, J., Sabatie- Gogová, A., Plutnar, J., Huclier-Markai, S., and Hermann, P. (2014) Thermodynamic and kinetic study of scandium (III) complexes of DTPA and DOTA: a step toward scandium radiopharmaceuticals, *Chemistry–A European Journal 20*, 7944-7955.

[3] Hawkes, D. J., Hill, D. L., Hallpike, L., and Bailey, D. L. (2005) Coregistration of structural and functional images, In *Positron Emission Tomography*, pp 161-177, Springer.

[4] Velikyan, I. (2014) Prospective of 68Ga-radiopharmaceutical development, *Theranostics 4*, 47-80.

[5] Price, E. W., and Orvig, C. (2014) Matching chelators to radiometals for radiopharmaceuticals, *Chemical Society Reviews 43*, 260-290.

[6] Spirlet, M. R., Rebizant, J., Desreux, J. F., and Loncin, M. F. (1984) Crystal and molecular structure of sodium aqua (1, 4, 7, 10-tetraazacyclododecane-1, 4, 7, 10-tetraacetato) europate (III) tetrahydrate Na+ (EuDOTA. H2O)-. 4H2O, and its relevance to NMR studies of the conformational behavior of the lanthanide complexes formed by the macrocyclic ligand DOTA, *Inorganic chemistry 23*, 359-363.

[7] Magerstädt, M., Gansow, O. A., Brechbiel, M. W., Colcher, D., Baltzer, L., Knop, R. H., Girton, M. E., and Naegele, M. (1986) Gd (DOTA): an alternative to Gd (DTPA) as a T1, 2 relaxation agent for NMR imaging or spectroscopy, *Magnetic resonance in medicine 3*, 808-812.

[8] De León-Rodríguez, L. M., and Kovacs, Z. (2007) The synthesis and chelation chemistry of DOTA− peptide conjugates, *Bioconjugate chemistry 19*, 391-402.

[9] Parker, D., Puschmann, H., Batsanov, A. S., and Senanayake, K. (2003) Structural analysis of nine-coordinate lanthanide complexes: steric control of the metal-water distance across the series, *Inorganic chemistry 42*, 8646-8651.

[10] Viola, N. A., Rarig, R. S., Ouellette, W., and Doyle, R. P. (2006) Synthesis, structure and thermal analysis of the gallium complex of 1, 4, 7, 10-tetraazacyclo-dodecane-N, N′, N ″, N‴-tetraacetic acid (DOTA), *Polyhedron 25*, 3457-3462.

[11] Woods, M., and Sherry, A. D. (2003) Synthesis and luminescence studies of aryl substituted tetraamide complexes of europium (III): a new approach to pH responsive luminescent europium probes, *Inorganic chemistry 42*, 4401-4408.

[12] Xiaohong, L., Ruizhou, Z., and Xianzhou, Z. (2010) Computational study of imidazole derivative as high energetic materials, *Journal of hazardous materials 183*, 622-631.

[13] Xu, X.-J., Xiao, H.-M., Ju, X.-H., Gong, X.-D., and Zhu, W.-H. (2006) Computational studies on polynitrohexaazaadmantanes as potential high energy density materials, *The Journal of Physical Chemistry A 110*, 5929-5933.

[14] Parr, R. G., and Yang, W. (1989) *Density-functional theory of atoms and molecules*, Vol. 16, Oxford university press.

[15] Yang, X. G., Chen, D., Wang, M., Xue, Y., and Chen, Y. Z. (2009) Prediction of antibacterial compounds by machine learning approaches, *Journal of computational chemistry 30*, 1202-1211.

[16] Burke, K. (2012) Perspective on density functional theory, *The Journal of chemical physics 136*, 150901.

[17] Frisch, M., Trucks, G., Schlegel, H., Scuseria, G., Robb, M., Cheeseman, J., Scalmani, G., Barone, V., Mennucci, B., and Petersson, G. (2009) gaussian 09, Gaussian, *Inc., Wallingford, CT 4*.

[18] Hay, P. J., and Wadt, W. R. (1985) Ab initio effective core potentials for molecular calculations. Potentials for K to Au including the outermost core orbitals, *The Journal of Chemical Physics 82*, 299-310.

[19] Hay, P. J., and Wadt, W. R. (1985) Ab initio effective core potentials for molecular calculations. Potentials for the transition metal atoms Sc to Hg, *The Journal of Chemical Physics 82*, 270-283.

[20] Schäfer, A., Horn, H., and Ahlrichs, R. (1992) Fully optimized contracted Gaussian basis sets for atoms Li to Kr, *The Journal of Chemical Physics 97*, 2571-2577.

[21] Wadt, W. R., and Hay, P. J. (1985) Ab initio effective core potentials for molecular calculations. Potentials for main group elements Na to Bi, *The Journal of Chemical Physics 82*, 284-298.

[22] Weigend, F., and Ahlrichs, R. (2005) Balanced basis sets of split valence, triple zeta valence and quadruple zeta valence quality for H to Rn: design and assessment of accuracy, *Physical Chemistry Chemical Physics 7*, 3297-3305.

[23] Weigend, F. (2006) Accurate Coulomb-fitting basis sets for H to Rn, *Physical chemistry chemical physics 8*, 1057-1065.

[24] Chai, J.-D., and Head-Gordon, M. (2008) Systematic optimization of long-range corrected hybrid density functionals, *The Journal of chemical physics 128*, 084106.

[25] Sebastian, S., Sylvestre, S., Jayabharathi, J., Ayyapan, S., Amalanathan, M., Oudayakumar, K., and Herman, I. A. (2015) Study on conformational stability, molecular structure, vibrational spectra, NBO, TD-DFT, HOMO and LUMO analysis of 3, 5-dinitrosalicylic acid by DFT techniques, *Spectrochimica Acta Part A: Molecular and Biomolecular Spectroscopy 136*, 1107-1118.

[26] Kohn, W., Becke, A. D., and Parr, R. G. (1996) Density functional theory of electronic structure, *The Journal of Physical Chemistry 100*, 12974-12980.

[27] Geerlings, P., De Proft, F., and Langenaeker, W. (2003) Conceptual density functional theory, *Chemical reviews 103*, 1793-1874.

[28] Parr, R. G., Szentpaly, L. v., and Liu, S. (1999) Electrophilicity index, *Journal of the American Chemical Society 121*, 1922-1924.

[29] Chattaraj, P. K., Lee, H., and Parr, R. G. (1991) HSAB principle, *Journal of the American Chemical Society 113*, 1855-1856.

[30] Coropceanu, V., Malagoli, M., da Silva Filho, D., Gruhn, N., Bill, T., and Brédas, J. (2002) Hole-and electron-vibrational couplings in oligoacene crystals: intramolecular contributions, *Physical review letters 89*, 275503.

[31] Cossi, M., Rega, N., Scalmani, G., and Barone, V. (2003) Energies, structures, and electronic properties of molecules in solution with the C- PCM solvation model, *Journal of computational chemistry 24*, 669-681.

[32] Foster, J., and Weinhold, F. (1980) Natural hybrid orbitals, *Journal of the American Chemical Society 102*, 7211-7218.

[33] Skelton, A. A., Agrawal, N., and Fried, J. R. (2015) Quantum mechanical calculations of the interactions between diazacrowns and the sodium cation: an insight into Na+ complexation in diazacrown-based synthetic ion channels, *RSC Advances 5*, 55033-55047.

[34] Pearson, R. G. (1985) Absolute electronegativity and absolute hardness of Lewis acids and bases, *Journal of the American Chemical Society 107*, 6801-6806.

[35] Pearson, R. G. (1987) Recent advances in the concept of hard and soft acids and bases, *J. chem. Educ 64*, 561.

[36] Lewis, D., Ioannides, C., and Parke, D. (1994) Interaction of a series of nitriles with the alcohol-inducible isoform of P450: Computer analysis of structure—activity relationships, *Xenobiotica 24*, 401-408.

[37] Zhou, Z., and Parr, R. G. (1990) Activation hardness: new index for describing the orientation of electrophilic aromatic substitution, *Journal of the American Chemical Society 112*, 5720-5724.

[38] Pathak, S., Srivastava, R., Sachan, A., Prasad, O., Sinha, L., Asiri, A., and Karabacak, M. (2015) Experimental (FT-IR, FT-Raman, UV and NMR) and quantum chemical studies on molecular structure, spectroscopic analysis, NLO, NBO and reactivity descriptors of 3, 5-Difluoroaniline, *Spectrochimica Acta Part A: Molecular and Biomolecular Spectroscopy 135*, 283-295.

[39] Parr, R. G., and Pearson, R. G. (1983) Absolute hardness: companion parameter to absolute electronegativity, *Journal of the American Chemical Society 105*, 7512-7516.

[40] Giannozzi, P., Baroni, S., Bonini, N., Calandra, M., Car, R., Cavazzoni, C., Ceresoli, D., Chiarotti, G. L., Cococcioni, M., and Dabo, I. (2009) QUANTUM ESPRESSO: a modular and open-source software project for quantum simulations of materials, *Journal of Physics: Condensed Matter 21*, 395502.

[41] Parker, D. (1990) Tumour targeting with radiolabelled macrocycle–antibody conjugates, *Chemical Society Reviews 19*, 271-291.

[42] Sigel, A., Sigel, H., and Sigel, R. K. (2016) *The Alkali Metal Ions: Their Role for Life*, Vol. 16, Springer International Publishing Switzerland, Switzerland.

CHAPTER 3

Chelation of DOTA with radiometal ions for radiolabeling: A DFT study

E. Frimpong, A. A. Skelton*, B. Honarparvar*

School of Pharmacy and Pharmacology, University of KwaZulu-Natal, Durban 4001, South Africa.

Corresponding author: Honarparvar@ukzn.ac.za (B. Honarparvar), Skelton@ukzn.ac.za (A.A Skelton)
School of Pharmacy and Pharmacology, University of KwaZulu-Natal, Durban 4001, South Africa. Tel.: +27 31 26084, +27 31 2608520.

Abstract

1, 4, 7, 10-tetraazacyclododecane-1, 4, 7, 10-tetracetic acid (DOTA) is an important chelator for radiolabeling of pharmaceuticals. The non-covalent interactions between DOTA chelator and Cu^{2+}, Sc^{3+}, In^{3+} and Ga^{3+} radiometal ions were performed using density functional theory with B3LYP functional and 6-311+G(2d,2p) and DGDZVP basis sets. Two different conformations were undertaken for the study, one where Ga^{3+} and Cu^{2+} ions were coordinated with four nitrogen atoms and two oxygen atoms of DOTA (conformation '**A**') while, In^{3+} and Sc^{3+} were coordinated with four nitrogen and four oxygen atoms (conformation '**B**'). Charge and ionic radius are two key factors that dictated the obtained electronic structure properties of the selected complexes. Interaction and relaxation energies, Gibbs free energies and entropies show that trivalent ion complexes, Ga^{3+}, In^{3+} and Sc^{3+}, are more stable than divalent Cu^{2+} ion complexes. As for the effect of ionic radius, In^{3+} with a larger ionic size than Ga^{3+}, shows a lower tendency to be chelated to DOTA. NBO analysis shows the charge transfer from the chelator to the radiometal ions resulting in reduced positive natural atomic charges for all ions. DOTA—Ga^{3+}, In^{3+} and Sc^{3+} complexes have also higher $\Delta E_{\text{LUMO-HOMO}}$ energies and chemical hardness values. DOTA—Cu^{2+} complex is found to be the least stable amongst the selected complexes. This study is a guide for radio-pharmaceuticals in finding the efficient optimal match between chelators and different radiometal ions for radiolabeling process.

Keywords: DOTA (1, 4, 7, 10-tetraazacyclododecane-1, 4, 7, 10-tetracetic acid); Chelator—radiometal ion interactions, Density functional theory (DFT); Natural bond orbital (NBO)

3.1   Introduction

The quest to find the optimal match between chelators and radiometal ions is one of the ongoing challenges in the field of radio pharmaceutical applications. Bifunctional chelators (BFCs) are used as ligands to deliver an isotope to a specific target *in vivo*[1, 2]. One terminus of a BFC coordinates a radiometal ion and the other is chemically bonded to the bioactive molecule. Macrocyclic chelators are preferred over their acyclic counterparts due to the thermodynamic stabilities of their radio metal complexes [3-8]. To achieve an efficient imaging or chelation therapy, the stability of chelator—ions complexes should be taken into consideration[9]. Several factors such as the nature of the ligand atoms, electron affinity of a metal and the ability of the chelators and ligands to charge transfer influence the stability of chelate—metal ion complexes [10, 11]. DOTA (1, 4, 7, 10-tetra acetic acid) is a macrocyclic chelator, which contains four pendant carboxylate arms connected to cyclen amines (**Figure 1**).
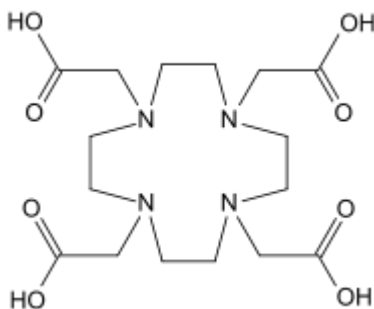
Figure 1.The structure of 1, 4, 7, 10-tetraazacyclododecane-1, 4, 7, 10-tetraacetic acid (DOTA).

Diversity of coordination number of radiometal ions involved in DOTA—radiometal ion complexes provides the possibility of having various complexes for radiolabeling. The coordination number for Cu^{2+} and Ga^{3+} is known to be 6 while for In^{3+} and Sc^{3+} has been reported to be 8[12-17]. DOTA complexes are known for their kinetic inertness *in vivo* and, hence, have been used extensively used for MRI imaging. DOTA—copper complexes are used for the imaging of tumors [18-22]. [111]Indium—DOTA complexes are applied for single photon emission tomography (SPECT) imaging [2]. In radiotherapy, the ^{68}Ga labeled DOTA is the most preferred choice due to its shorter half-life [23]. The present study investigates the complexation of DOTA with selected radiometal ions (Cu^{2+}, Sc^{3+}, In^{3+} and Ga^{3+}) with different conformational possibilities using density functional theory (DFT). Knowing that charge

and ionic radius are major factors that should govern the electronic structure properties that contribute to chelation, the DFT-based quantities were compared with experimental binding constants[2]. Another goal of this study is to investigate the possible competition between radiometals and alkali metal ions, found in the body, upon complexation with DOTA. To address these targets, stability of the various complexes were evaluated in terms of interaction energies, thermochemical properties, NBO analysis, frontier orbital analysis and DFT-based electronic structure quantities such as electron affinity (EA), ionization potential (IP), chemical softness (S) and hardness (η). The outcome of this study is helpful in the selection the suitable and optimal radiometal ions for the specific chelator for radiopharmaceuticals.

3.2   Computational details

Full geometry optimizations of all the selected DOTA─radiometal ion complexes and electronic structure calculations were carried out using Gaussian 09 program [24]. Density functional theory with the B3LYP functional [25-27] and 6-311G+(2d, 2p) basis set was employed for DOTA while DGDPVZ [28, 29] was used for the radiometal ions. BSSE calculations were performed to assess the effectiveness of the chosen basis sets. Interaction energies (E_{int}) were calculated as follows:

$$E_{int} = E_{DOTA-ion\ complex} - E_{DOTA} - E_{ion} \tag{1}$$

The ions described in the equation are Cu^{2+}, Ga^{3+}, In^{3+} or Sc^{3+}.

Relaxation energies (E_{relax}) were calculated by subtracting the complexation energies (unrelaxed) from the interaction energies (relaxed). After the geometry optimization of the DOTA─cation complexes, the cation was removed from DOTA and single point energy of DOTA in the same configuration was performed. Secondly, a further geometry optimization of the DOTA was performed to enable DOTA to relax. The difference in energies between the two previously explained cases is called the relaxation energy, which provides a measure of how the ion affects the conformation of the DOTA. To account for long range and dispersion contributions to the E_{int} values obtained for the various complexes, further calculations were performed using the ωB97XD density functional. Interatomic short-range distances ≤ 2.5Å between the ions and the heteroatoms have been recorded.

Natural bond orbital (NBO) analysis were performed at the B3LYP level of theory with 6-311G+ (2d,2p) and DGDPVZ basis sets using NBO program implemented in Gaussian 09 program; this was used to understand natural atomic charge distribution and charge transfer between DOTA and the investigated ions (Cu^{2+}, Ga^{3+}, In^{3+} and Sc^{3+}). To evaluate the donor and acceptor interactions in each of the complex, the second-order Fock matrix within NBO basis was employed [30]. Second perturbation theory confirms whether there is an electron donation from one orbital to another. This electron donation results in the stabilization energy (E^2):

$$E^2 = \frac{q_i F(i,j)^2}{\varepsilon_j - \varepsilon_i} \tag{3}$$

Where q_i is the orbital occupancy, ε_i, ε_j are diagonal elements and $F_{i,j}$ is the off diagonal NBO Fock matrix element.

Atoms in each complex were categorized based on their proximity with ions ($\leq$2.5Å range) after geometry optimizations. The DFT based reactivity descriptors calculations were preformed using the following equations [31-34]:

Chemical hardness is defined as:

$$\eta = \frac{IP - EA}{2} \tag{4}$$

and softness,

$$S = \frac{1}{2\eta} \tag{5}$$

Ionization potential (IP) was obtained by the usage of energy differences between radical cation, Ec and the respective neutral molecule $IP = E_c - E_n$. Electron affinity (EA) was calculated by, the energy differences between a radical anion, E_a and the respective neutral molecule, $EA = E_a - E_n$. The term "neutral" denotes the standard charge state, for instance, the ions have +1 charge and cationic and anionic species have +2 and 0 charges, respectively. Using normal mode analysis, thermodynamic properties (enthalpy, free energy and entropy with different translational, vibrational and rotational contributions) were calculated. To assess the solvent effect on the DOTA complexation with radio metals, Polarizable Continuum Model (PCM), using the integral equation-formalism polarizable continuum model (IEF-PCM) was employed. Finally, eigenstate energies of the highest occupied

molecular orbital (HOMO) and the lowest unoccupied molecular orbital (LUMO) of all the DOTA—ion complexes were calculated making use of the same level of theory.

3.3   Results and discussions

Classifications of different atomic groups involved in the DOTA—ion complexes were considered in terms of their position and connectivity in relation to different functional groups. Assessment was performed on the contributions of various functional groups to the geometries and electronic structures properties of DOTA—radiometal ions complexes (**Figure 2**).

3.3.1   Conformational analysis

Four carboxylic pendant arms (—COOH) of DOTA, offer diverse conformational possibilities of DOTA—radiometal ions complexes. The geometry optimization was performed on the three experimentally derived crystal structures (**Figure 2**). It is notable that, the crystal structure of DOTA complexed with In^{3+} was modified because it had a quinazoline unit attached to it.   First, the crystal structure of DOTA, where four pendant arms were in close proximity with Sc^{3+} was used as a starting structure and replaced with Cu^{2+}, Ga^{3+} and In^{3+} for further geometry optimization of other complexes (**Figure 2a**). Secondly, the crystal structure of DOTA, where two pendant arms were in close proximity with Ga^{3+} [12], was used as a starting structure and replaced with Cu^{2+}, Sc^{3+} and In^{3+} for further geometry optimization of other complexes (**Figure 2b**). Lastly, the crystal structure of DOTA, where three pendant arms were in close contact with In^{3+} [35] was geometry optimized and then the In^{3+} ion was replaced with Cu^{2+}, Ga^{3+}, In^{3+} and further geometry optimized (**Figure 2c**).
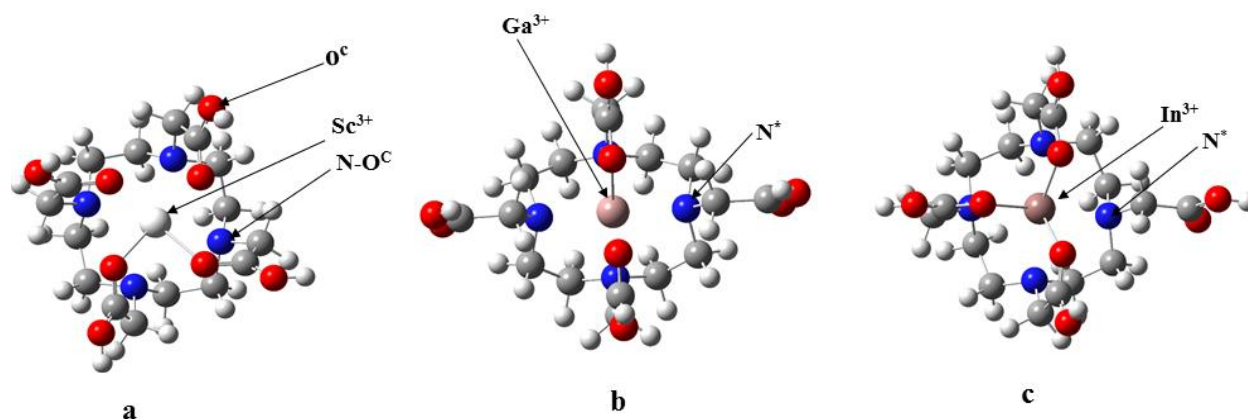
Figure 2. **a**: The optimized complexes with the DOTA—Sc^{3+} crystal structure as the starting structure ; **b**: denotes the geometry optimized complexes from the DOTA—Ga^{3+} crystal structure as the starting structure **c**: The optimized structures from DOTA—In^{3+} crystal structure as the starting structure. Carbonyl oxygen in close contact with an ion (O^C). Nitrogen and carbonyl oxygen in close contact with an ion (N). Nitrogen and carbonyl oxygen not in close contact with an ion (N*).

The relative energies for the different DOTA— radiometal ion complexes are reported in **Table 1**. The complex conformations starting from the crystal structure of DOTA— Sc^{3+} [35] had more negative energies and were assigned as the reference (**a** in **Table 1** and **Figure 2**); the relative energies for the other two conformational possibilities (**b** and **c** in **Table 1** and **Figure 2**) were calculated with respect to the reference.

Table 1. The relative energies (kcal mol^{-1}) for the selected DOTA—radiometal ion complexes. The structures of **a**, **b** and **c** are demonstrated in **Figure 2**.

Complexes	$\Delta E_{relative}$ Crystal structure [a] (kcal mol^{-1})	$\Delta E_{relative}$ Crystal structure [b] (kcal mol^{-1})	$\Delta E_{relative}$ Crystal structure [c] (kcal mol^{-1})
DOTA—Cu^{2+}	0 (6)	17.25 (6)	4.44 (6)
DOTA—Sc^{3+}	0 (8)	67.38 (6)	19.44 (7)
DOTA—In^{3+}	0 (8)	53.30 (6)	13.17 (7)
DOTA—Ga^{3+}	0 (6)	26.94 (6)	3.57 (6)

Parenthesis show the co-ordination number in each complex, which was assessed by considering heteroatom-ion distances ≤ 2.5 Å.

It is noticed that the presence of Sc^{3+} and In^{3+} made the complex to prefer to be coordinated to 8 heteroatoms while Cu^{3+} and Ga^{3+} prefer to be coordinated to 6 heteroatoms; that is, in structure **a**,

40

DOTA—Sc^{3+} and DOTA—In^{3+} have 8 coordination and have higher $\Delta E_{relative}$ values for both structures **b** and **c**, with coordination numbers of 6 and 7, respectively. Conversely, for DOTA—Cu^{2+} and DOTA—Ga^{3+} complexes, all structures (**a, b** and **c** in **Figure 2**) have coordination number of 6 and lower $\Delta E_{relative}$ values than that of DOTA—Sc^{3+} and DOTA—In^{3+} complexes.

It is evident in **Table 1** that, even though some complexes had the same co-ordination numbers for **a, b,** and **c**, there were differences in the energy values; this is due to the fact that, the distances between O^C and N atoms and the Cu^{2+}, Sc^{3+}, In^{3+} and Ga^{3+} ions varied (**Table 5**).

Considering the different conformational possibilities for **a** in **Figure 2**, it is noticed that after replacement of Sc^{3+} with the other radiometal ions (Cu^{2+}, Ga^{3+}, In^{3+}) and further geometry optimizations, two different conformations ('**A**' and '**B**') were identified. There was one conformation for DOTA—Cu^{2+} and DOTA—Ga^{3+} ('**A**') with four nitrogen and two oxygen atoms interacting with the ions and another one ('**B**') with four nitrogen atoms and four oxygen atoms in close contact with In^{3+} and Sc^{3+} (**Figure 3**).
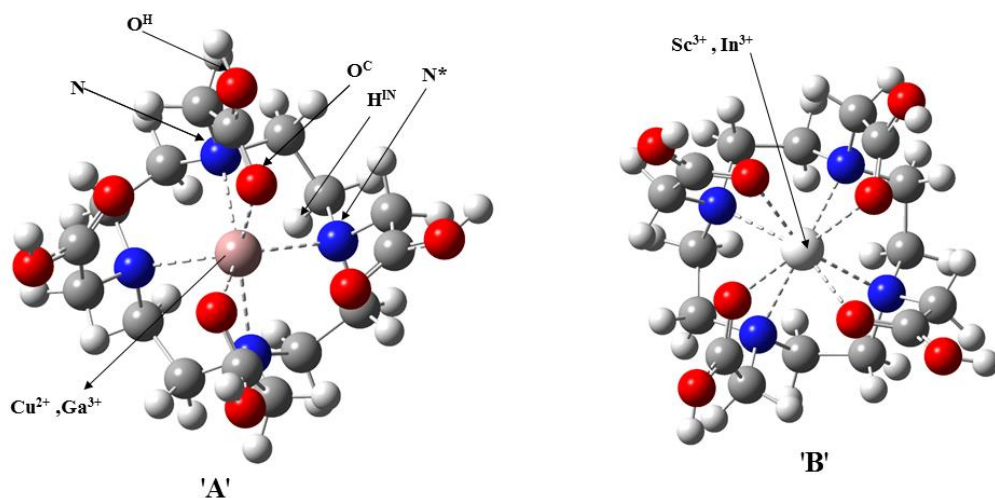
Figure 3. Conformation of the DOTA—ion complexes: DOTA—Cu^{2+}, DOTA—Ga^{3+}, DOTA—In^{3+} and DOTA—Sc^{3+}. In this diagram, the intermolecular distances between DOTA's heteroatoms interacting with the selected radiometal ions are marked by dotted lines. '**A**': DOTA—Cu^{2+} and DOTA—Ga^{3+} have 4N and 2O in close proximity with ions. '**B**': DOTA—In^{3+} and DOTA—Sc^{3+} have 4N and 4O atoms within (≤ 2.5 Å) range. Carbonyl oxygen (O^C) is in close contact with an ion. Nitrogen and carbonyl oxygen atoms are in close contact with an ion (N). Nitrogen is in close contact with an ion but carbonyl oxygen is not in close proximity (N^*).

3.3.2 Interaction and relaxation energies

In this section, the interaction energies (E_{int}), relaxation energies (E_{relax}) and basis set superposition error (BSSE) of the DOTA—radiometal ion complexes are analyzed (**Table 2**) to understand the binding of DOTA with the selected ions. The E_{int} values indicate the strength of the possible non-covalent interactions that contribute to the complexation of DOTA with radiometal ions to produce stable complexes.

Table 2. The interaction, relaxation and BSSE energies of the DOTA—radiometal ion complexes in vacuum and solvent obtained by B3LYP/6-311G+(2d,2p) and DGDPVZ basis set for ions. To account for the effect of dispersion on the various complexes, E_{int} using ωB97XD functional is also reported.

Complex	E_{int} (kcal mol^{-1})		E_{relax} (kcal mol^{-1})	E_{BSSE} (kcal mol^{-1})
	B3LYP	ωB97XD		
DOTA—Cu^{2+}	-412.84 (-202.10)	-406.93	41.00	11.45
DOTA—Sc^{3+}	-680.93 (-152.89)	-677.27	70.89	24.75
DOTA—In^{3+}	-694.48 (-378.93)	-699.89	61.94	16.99
DOTA—Ga^{3+}	-820.13 (-498.89)	-814.33	65.58	7.47

Parentheses show the values for water medium.

According to **Table 2**, DOTA—Ga^{3+} has the most negative interaction energy while the least E_{int} is recorded by DOTA—Cu^{2+} complex. Relaxation energies (E_{relax}) provide helpful insight into the effect of the ions on inducing specific DOTA conformations. Even though Ga^{3+} and In^{3+} are group III elements, significant differences between their E_{relax} values were obtained (**Table 2**) which implies each radiometal ion induces a specific conformation on DOTA chelator. To account for the long range and dispersion interactions, the geometry optimization of the complexes were performed using the ωb97XD functional and the interaction energies are also reported in **Table 2.** It is significant to point out that the observed differences between interaction energies obtained by B3LYP and ωB97XD density functionals could be attributed to different factors contributing to complexation since dispersion should have a less significant effect on the obtained large interaction energies (**Table 2**). In other words, it is assumed that the observed ranges of Eint values are much stronger than intermolecular interactions and should be assumed as bonding interactions. It is notable that the interaction energies obtained with both B3LYP and ωb97XD functionals show the same trend. Thus, the results obtained with B3LYP are qualitatively similar.

The interaction energies follows the order DOTA—Ga^{3+}>DOTA—In^{3+}>DOTA—Sc^{3+}> DOTA—Cu^{2+}, which can be justified based on the different characteristics of each ion. In other words, Ga^{3+} is in the same group as In^{3+} with a smaller atomic radius, which leads to stronger interactions between Ga^{3+} and DOTA. This is in agreement with results of our previous work [36], where it was found that the strength of interactions within DOTA—alkali metal ion complexes increased up the group of the periodic table. The difference in interaction energies between Sc^{3+} and Cu^{2+} is due to their charge, Sc^{3+} being +3 forms stronger interactions with DOTA than Cu^{2+} with a +2 charge.

To gain an understanding of how structural geometries and interaction energies of DOTA—ion complexes may be altered in water, E_{int} of the various complexes in aqueous medium (water) were also calculated. It can be realized that in the presence of bulk water, E_{int} values for all the complexes are considerably less negative and less stable than in vacuum; hence, it can be inferred that the possible interactions of water with radiometal ions creates competitions and interferes with the chelation of radiometal ions with the DOTA and consequently decreases the stability of the DOTA—ion complexes. It can be also observed that in water medium, DOTA—Cu^{2+} complex, which has the least negative E_{int} in vacuum, has more negative E_{int} than DOTA—Sc^{3+} indicating that the water solvation affects the triply charged Sc^{3+} to a greater extent than the doubly charged Cu^{2+}. The BSSE energies recorded for the various DOTA—ion complexes were higher than what we observed for DOTA—alkali metals in our previous study[36]. This could be attributed to higher E_{int} values obtained by the various complexes compared to the ones recorded between the ligand and alkali metals.

3.3.3 Thermodynamic properties

To gain an insight into the favorability of DOTA—ion complexation, the analysis of enthalpies, Gibbs free energies, entropy and its individual contributions (translational, rotational, and vibrational) of the radiometal ions complexed with DOTA are discussed (**Table 3**).

Table 3. The enthalpies, Gibbs free energies, entropy and its individual contributions (Translational, rotational, and vibrational) of the radiometal ions complexed with DOTA obtained by B3LYP/6-311G+(2d,2p) and DGDPVZ basis sets.

Complex	ΔH (kcal mol^{-1})	ΔG (kcal mol^{-1})	ΔS (cal mol^{-1} K^{-1})	ΔS_{Rot} (cal mol^{-1} K^{-1})	ΔS_{Trans} (cal mol^{-1} K^{-1})	ΔS_{Vib} (cal mol^{-1} K^{-1})
DOTA—Cu^{2+}	-410.24 [-197.79]	-398.35 [-185.92]	-39.88 [-39.84]	-0.17 [-0.29]	-37.91 [-37.91]	-1.80 [-1.65]
DOTA—Sc^{3+}	-678.01 [-149.63]	-662.59 [-133.89]	-51.72 [-52.81]	-0.16 [-0.32]	-37.02 [-37.02]	-14.53 [-15.47]
DOTA—In^{3+}	-691.54 [-374.26]	-676.87 [-359.26]	-49.20 [-50.30]	-0.10 [-0.26]	-39.39 [-39.39]	-9.71 [-10.65]
DOTA—Ga^{3+}	-816.61 [-492.87]	-802.32 [-477.73]	-47.91 [-50.77]	-0.22 [-0.37]	-38.14 [-37.87]	-9.55 [-12.62]

Brackets([]) indicate results obtained in aqueous medium.

Table 3 shows that for all cases, **ΔH** values of the complexes are slightly less negative than E_{int}. Considering the equation $\Delta G = \Delta H - T\Delta S$, it is clear that entropy acted against DOTA—ion complexation because negative entropies are recorded for each complex. Vibrational contributions (ΔS_{vib}) to entropies are more negative for the complexes involving trivalent ions than the divalent Cu^{2+} complexes, which is due to the stronger intermolecular interactions within the DOTA—trivalent ion complexes than divalent case (Cu^{2+}), supported by the obtained E_{int} values (**Table 2**). The effect of implicit solvation on the enthalpies, Gibbs free energies and entropies was also investigated. Overall, according to the obtained interaction energies (**Table 2**) and the thermochemical quantities (**Table 3**), the formation of DOTA—Ga^{3+} and DOTA—In^{3+}, in both vacuum and water are found to be significantly more favorable than the other studied DOTA—radiometal ion complexes. Considering all the thermochemical quantities obtained in water medium for various complexes, it can be realized that the complexation of DOTA with radiometal ions is less favorable and less stable in aqueous medium than in vacuum.

3.3.4 Comparison of experimental and theoretical binding constants

The theoretical and experimental Gibbs free energies (ΔG_{theo} and ΔG_{exp}) of the selected DOTA—radiometal ion complexes [2, 37] are related to the experimental binding constants (logK$_{exp}$) using Vant Hoff equation ($\Delta G = -RT \ln K$) [38]. Experimental ΔG_{exp} and theoretical binding constants (logK$_{theo}$) were calculated at the standard temperature (298K) and molar gas constant R (8.315 Jk^{-}

^{1}mol^{-1}). The experimental and theoretical values of both the Gibbs free energies and binding constants are reported in **Table 4**.

Table 4 The theoretical and experimental Gibbs free energies (ΔG_{theo} and ΔG_{exp}) with their corresponding binding constants (logK$_{theo}$ and logK$_{exp}$)^2.

Complex	ΔG_{theo} (kcal mol^{-1})	ΔG_{exp} (kcal mol^{-1})	logK$_{exp}$ [2]	logK$_{theo}$
DOTA―Cu^{2+}	-398.35	-13.15	22.70	11.21
DOTA―Sc^{3+}	-662.59	-15.64	27.00	11.89
DOTA―In^{3+}	-676.87	-13.85	23.90	11.79
DOTA―Ga^{3+}	-802.32	-12.34	21.30	11.84

First, the experimentally measured ΔG_{exp} are considerably more negative than the theoretical ΔG_{theo} values and the theoretical binding constant values are higher than the experimental binding constants. However, a comparison of the theoretical vs experimental trends within the ion complexes should be informative for understanding the factors that contribute to complex stabilities.

The theoretical values for both DOTA―Cu^{2+} and DOTA―Ga^{3+} complexes deviated from the experimental trend due to the fact that they have the lowest and highest E$_{int}$ values, respectively (**Table 2**). The difference between the calculated binding constants (logK$_{theo}$) with experiment (logK$_{exp}$) [2, 37] might be due to the fact that at specific temperature, pH and solvent, which affect the stability constants, were not included in our calculations.

3.3.5   Interatomic distances

To assess the extent of intermolecular interactions between DOTA and radiometal ions, the average interatomic distances between the radiometal ions and DOTA heteroatoms in the optimized complexes are measured in vacuum and water media (**Table 5**).

Table 5. The average short-range interatomic distances between radiometal ions and DOTA's heteroatoms in the optimized structures obtained by the B3LYP density functional with 6-311G+ (2d, 2p)/DGDPVZ basis sets. Heteroatom-ion distances ≤ 2.5 Å were considered as the short-range interatomic distances for the selected complexes. O^C and N are presented in **Figure 3a**.

Complex	O^C —ion (≤ 2.5Å)	N—ion (≤ 2.5Å)
DOTA—Cu^{2+}	2.38 [2.48]	2.17 [2.15]
DOTA—Sc^{3+}	2.22 [2.46]	2.24 [2.25]
DOTA—In^{3+}	2.33 [2.44]	2.47 [2.35]
DOTA—Ga^{3+}	2.04 [2.05]	2.25 [2.21]

Brackets indicate bond distances between heteroatoms of DOTA and radiometal ions in water.

As shown in **Table 5**, the average interatomic O^C—ion distances are shorter within the trivalent ions complexes, DOTA— Sc^{3+},In^{3+} and Ga^{3+} than that of DOTA—Cu^{2+}; this could be a reason of more negative E_{int} values obtained for trivalent ions complexes than DOTA—Cu^{2+} (**Table 2**). It is significant to point out that the shorter distances of O^C—ions in compared with the N-O^C—ions for within the trivalent ions complexes implies the stronger interactions between O^C—ions than N—ion interactions within these complexes. In contrast with trivalent ions complexes, in the case of DOTA—Cu^{2+}, have shorter average N—ion distances which accounted for a more negative energy E_{int} values (**Table 2**).

3.3.6   Comparison of the optimized and experimental x-ray structures

To further validate the theoretically optimized structures of DOTA—radiometal ion complexes with experimentally reported conformations, the geometries of the complexes (**Figures 4a** and **4d**) were compared with experiment (**Figures 4b**, **4c**, **4e** and **4f**) [12-16]. This analysis is also helpful to assess the strength of intermolecular interactions between DOTA and radiometal ions.

In **Figure 4**, the conformation 'A', with six hetero-atoms (4 nitrogen and 2 oxygen atoms) interacting with the ions (**a**), while conformation '**B**', with four nitrogen and four oxygen atoms in close proximity with ions (**d**). The geometry of our optimized structures are in good agreement with x-ray crystal structures of the selected complexes. DOTA—Cu^{2+} (distorted octahedron), DOTA—Ga^{3+} (distorted octahedron), DOTA—In^{3+} (square antiprism) and DOTA—Sc^{3+} (square antiprism) [12-16] are demonstrated in **Figure 4** (**b, c, e** and **f**).
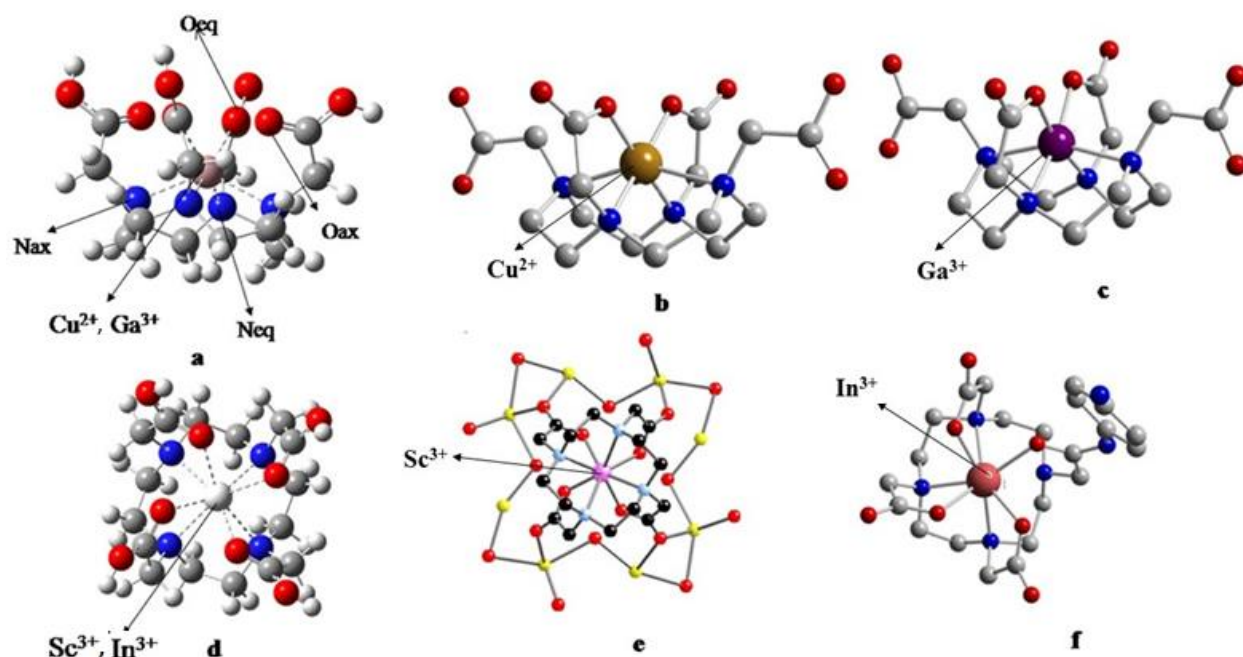
Figure 4. a: DOTA―Cu^{2+} and DOTA―Ga^{3+} theoretically optimized structures, **b:** DOTA―Cu^{2+} experimental x-ray structure, **c**: DOTA―Ga^{3+} experimental x-ray structure, **d**: DOTA―In^{3+} and DOTA―Sc^{3+} theoretically optimized structures, **e**: DOTA―Sc^{3+} experimental x-ray structure, **f**: DOTA―In^{3+} experimental x-ray structure, O_{eq}: Equatorial Oxygen; O_{ax}: axial Oxygen; N_{eq}: equatorial nitrogen; N_{ax}: axial nitrogen.

The comparison between our theoretical optimized structures and experimental x-ray structures is presented in **Table 6**.

Table 6. Average theoretical short-range interatomic distances (Å) between ions and N, O atoms of DOTA ($\leq$ 2.5 Å) obtained by the B3LYP method with 6-311G+ (2d, 2p) and DGDPVZ basis sets for ions. Parentheses show experimental results[16, 39].

Complex	N_{eq}―ion	N_{ax}―ion	O_{eq}―ion	N―ion	O―ion
DOTA―Cu^{2+}	2.16 (2.22)	2.18 (2.22)	2.38 (1.97)	―	―
DOTA―Sc^{3+}	―	―	―	2.24 (2.44)	2.24 (2.15)
DOTA―In^{3+}	―	―	―	2.47 (2.37)	2.33 (2.18)
DOTA―Ga^{3+}	2.23 (2.12)	2.27 (2.13)	2.04 (1.94)	―	―

Parentheses show the short-range interatomic distances (Å) between heteroatoms of DOTA and radiometal ions in complexes in water.

Even though Ga^{3+} and In^{3+} are in the same group of the periodic table (group III), the differences in their ionic radii and charge densities dictates their co-ordination chemistry. Ga^{3+} has an ionic radius of 0.65 Å [40] and has a co-ordination number of six in its complexes[41] while In^{3+} with an ionic radius 0.92 Å [40] has a co-ordination number of seven or eight within complexes [16, 42-44]. For Cu^{2+}, with a co-ordination number of six [13], two apical donor atoms are weakly bonded to the Cu^{2+} in a distorted octahedral conformation, due to John-Teller distortion within DOTA—Cu^{2+} complexes. Elongated Cu^{2+}—N_{ax} average bond length (2.18 Å) are in agreement with the expected Jahn-Teller effects caused by the d^9 configuration. Reisen *et al* reported that copper (II) coordinates DOTA using four of its nitrogen atoms and two oxygen atoms from the carboxylic arms. The angle between the metal ion and the two coordinating oxygen atoms was recorded at 88.7°. In our DFT calculated structures, the angle between two equatorial oxygen atoms coordinating with the ion was 80.85°, which is close to the experimentally observed values for *cis* nitrogen atoms (82.31° and 81.09°). Trans nitrogen ion bond angles were 152.59° and 104.96°. We observed 83.77° and 82.81° for *cis* nitrogen atoms while *trans* nitrogen atoms were at 142.05° and 143.93°, respectively[13].

Ga^{3+} coordinates DOTA using four of its nitrogen and two oxygen atoms from the carboxyl arms as reported by Viola-Villegas *et al.*[12]. An observed bond angle of 85.3° was recorded between the coordinated equatorial oxygen atoms and the metal ions. In our study, we observed 83.18°. Experimental results showed that the angles between *cis* nitrogen atoms and the metal ion (Ga^{3+}) angles fell within this range (82.3° to 84.19°). Our theoretical study recorded values within 80.33° and 81.6° range [39]. According to HSAB principle [2], Ga^{3+} which is a hard acid that prefers to coordinate hard ligand donors (carboxylate-oxygen atoms and amine nitrogen atoms); consequently, DOTA—Ga^{3+} complex in this study recorded the shortest O—ion interatomic distances. Previous structural studies have confirmed that the preferred co-ordination number for Indium (III) is 7 or 8 [35, 45, 46]. For DOTA—In^{3+} complex, the obtained theoretical geometric parameters are in good agreement with literature. Sc^{3+} has a co-ordination number of eight [14, 47]. Bombieri *et al* reported an octa-coordinate square prismatic geometry for a single crystal of [Sc(DOTA)]⁻ [14]. Previously, researchers reported similar square antiprism geometry for this complex [48-50]. Our theoretically optimized conformations had Sc^{3+} ion coordinated the DOTA with four nitrogen and four oxygen atoms (**Figure 3**).

3.3.7 Natural Bond Orbital (NBO) analysis

The natural atomic charge exchange upon complexation and charge transfer within the DOTA—radiometal ion complexes affects the interaction of radiometal ions with DOTA. Natural bond orbital (NBO) [51] analysis was performed to investigate the natural atomic charges (NACs) and the possible intermolecular orbital charge transfer within the studied complexes using second perturbation theory.

3.3.8 Natural atomic charge analysis (NAC)

Natural atomic charge estimation is of importance for molecular systems because atomic charge affects the electronic structure, dipole moment and other properties of the molecule. To evaluate the atomic charge exchange between DOTA and the selected radiometal ions upon complexation, NAC analysis [51, 52] was performed and these values for each sub-category is summarised in **Table 7**. The atoms in all the complexes were categorized into groups (**Figure 2**) and the average natural atomic charges in vacuum and water media are reported.

Table7. Natural atomic charges of classified hetero-atoms of DOTA obtained by B3LYP/6-311+G(2d,2p) and DGDPVZ basis set for ions. The numbers in parentheses represent the number of atoms within the specific group shown in **Figure 2**.

Atoms	Free DOTA	DOTA—Cu^{2+}	DOTA—Sc^{3+}	DOTA—In^{3+}	DOTA—Ga^{3+}
Ions		0.991	1.641	1.972	1.801
		[0.996]	[1.645]	[1.970]	[1.816]
O^C	-0.640	-0.613	-0.678	-0.693	-0.713
	[-0.665] (4)	[-0.620] (2)	[-0.673] (4)	[-0.689] (4)	[-0.711] (2)
N	-0.567	-0.555	-0.620	-0.622	-0.575
	[-0.574] (4)	[-0.556] (4)	[-0.621] (4)	[-0.689] (4)	[-0.639](4)
H^{IN}	0.186	0.222	0.230	0.230	0.236
	[0.193] (16)	[0.228] (16)	[0.231] (16)	[0.233] (16)	[0.240] (16)

Brackets([]) indicate the NAC values obtained in water.

Table 7 lists the main atom classification, sub-categories and average of the natural atomic charges for various atoms types in each complex. As for the atomic charge exchange between DOTA and radiometal ions upon complexation, the complexes with initial charge of +2 for Cu^{2+} and +3 for Sc^{3+},

In^{3+} and Ga^{3+}, before complexation, become less electron deficient after complexation. In the case of DOTA—Cu^{2+} complex, the ion had a deficit of (2e$^-$) but became less deficient (0.991e$^-$) after its interaction and complexation with the chelator. A similar reduction was observed in the positive charges for the trivalent ions, *i.e,* Ga^{3+} became less deficient (1.801e$^-$) upon complexation with DOTA. In^{3+} and Sc^{3+} have 1.972e$^-$ and 1.641e$^-$ after complexation, respectively. NAC values of N and O^C atoms within the trivalent ions complexes were more negative than the divalent ion complex; this could be attributed to the strong interactions that took place between DOTA and radiometal ions for the trivalent ions complexes. The observed charge reduction, particularly for In^{3+} and Ga^{3+}, which are in the same group of the periodic table, could be a reason for the stronger interaction energies observed in **Table 2**. The hydrogen atoms attached to the carbons which formed the ring (H^{IN}), served as the electron resource in each of the complex with the higher average (H^{IN}) values compared to the one recorded for free DOTA. The electron density transfer from DOTA to the radiometal ions upon complexation will be discussed using second order perturbation theory in the next section (**Table 8**).

3.3.9   Second perturbation stabilization energies

The second-order Fock matrix was presented to evaluate the donor–acceptor interactions in the system [147, 148]. Larger E^2 values imply greater charge transfer between electron donors and acceptors [53]. Charge transfer between DOTA and the investigated ions, as well as within the chelator, are presented in **Table 8**. A description of charge transfer (the highest stabilization energy values) that occurs from the DOTA molecule to the cations and this is also demonstrated in **Figure 5**, where curved arrows depict the direction of charge transfer.

Table 8. Second order pertubation theory analysis of Fock matrix in NBO basis of selected calculated values in each DOTA—ion complex obtained by B3LYP/6-311G+(2d,2p) and DGDPVZ basis sets for ions.

Complexes	Donor	Acceptor	E^2 (kcal mol^{-1})
From DOTA to ions			
DOTA— Cu^{2+}	LP (O^C)	LP* (Cu^{2+})	6.18
DOTA— Sc^{3+}	LP (O^C)	LP* (Ga^{3+})	24.05
DOTA— In^{3+}	LP (O^C)	LP* (In^{3+})	20.74
DOTA— Ga^{3+}	LP (O^C)	LP* (Sc^{3+})	30.29
Within DOTA			
DOTA—Cu^{2+}	LP (O^H)	σ* (C-O)	28.72
DOTA— Sc^{3+}	LP (O^H)	σ* (C-O)	64.96
DOTA—In^{3+}	LP (O^H)	σ* (C-O)	46.05
DOTA— Ga^{3+}	LP (O^H)	σ* (C-O)	73.83
Free DOTA	LP (O^H)	σ* (C-O)	56.21

The observed depletion of NAC charges of the ions (**Table 7**) is due to charge transfer from DOTA to the ions. According to the stabilization energies (E^2), shown in **Table 8** and **Figure 5**, the highest stabilization energy values for electron transfer from DOTA to ions and charge transfer occur from the LP (O^C) atom of DOTA to the LP* of the radiometals ions. The stabilization energies are larger in the complex involving trivalent Ga^{3+}, In^{3+} and Sc^{3+} ions (ranging from 20.74 to 30.29 kcal mol^{-1}) than the divalent DOTA—Cu^{2+} complex (6.18 kcal mol^{-1}); *i.e.,* the order is as follows: DOTA—Ga^{3+}>DOTA—In^{3+}>DOTA—Sc^{3+}>DOTA—Cu^{2+}, which is consistent with the observed trend for interaction energies (**Table 2**). The presence of different ions within the DOTA—ion complexes can affect the charge transfer within DOTA. In all the studied cases, there is a charge transfer within DOTA, from the LP of the O^H atom to the σ*(C-O^C) of the same arm of DOTA in each complex.
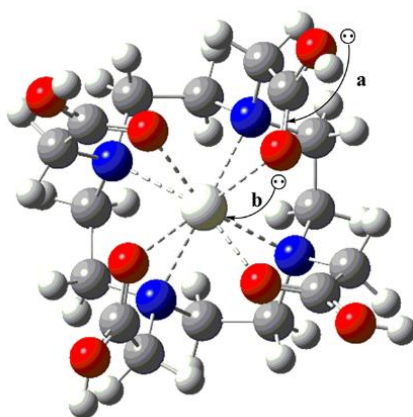
Figure 5. A presentation of the charge transfer for DOTA—radiometal ion complexes derived from NBO analysis using second order perturbation theory. The curved arrows (**a** and **b**) point the direction of charge transfer. **a**: LP (O^H) $\rightarrow$ σ^* (C-O^C) **b**: LP (O^C) $\rightarrow$ LP* (Ion).

The stabilization energy within DOTA follows the order: DOTA—Ga^{3+}> DOTA—Sc^{3+}> DOTA—In^{3+}> DOTA—Cu^{2+}; this is caused by the contribution of charge for +3 charge ions compared to the divalent Cu^{2+} ion. Overall, the result of the second order perturbation theory reveals the charge transfer from O^C of DOTA to the radiometal ions in the complexes. A similar observation was made from our previous works where we evaluated the interaction between diazacrown and the sodium cation [53] and the interaction between DOTA and alkali metal ions discussed in the previous chapter.

3.3.10   Analysis of frontier molecular orbitals

The highest occupied molecular orbitals (HOMO) and the lowest unoccupied molecular orbitals (LUMO) are known as frontier molecular orbitals. The energy difference between the two frontier molecular orbitals ($\Delta E_{LUMO-HOMO}$) [54, 55], is used to evaluate the complex stability of the selected DOTA—radiometal ion complexes. The E_{HOMO} and E_{LUMO} energy eigenvalues and $\Delta E_{LUMO-HOMO}$ for the free ions, DOTA and the DOTA—ion complexes are listed in **Table 9**.

Table 9. The energy eigenvalues of the frontier molecular orbitals (E_{HOMO}, E_{LUMO}) for the selected metal ions and DOTA—radiometal ion complexes obtained by B3LYP/6-311G+(2d,2p) and DGDPVZ basis sets for ions.

SYSTEM	E_{HOMO}/eV	E_{LUMO}/eV	$\Delta E_{LUMO-HOMO}$/eV
Cu^{2+}	-32.87	-28.25	4.62
Sc^{3+}	-68.58	-30.58	37.99
In^{3+}	-51.89	-31.31	20.57
Ga^{3+}	-57.97	-35.64	22.33
Free DOTA	-8.66	-3.96	4.70
DOTA—Cu^{2+}	-4.11	-3.81	0.31
DOTA— Sc^{3+}	-10.21	-4.75	5.46
DOTA—In^{3+}	-10.15	-4.47	5.68
DOTA— Ga^{3+}	-9.29	-3.90	5.39

Both the E_{HOMO} and $\Delta E_{LUMO-HOMO}$ values of the free radiometal ions follow the order: $Sc^{3+}> Ga^{3+}> In^{3+} > Cu^{2+}$; that is, the divalent Cu^{2+} has lower values compared to the trivalent ions, which could be attributed to the higher chemical hardness values obtained (**Table 9**). The higher the $\Delta E_{LUMO-HOMO}$ value of a system, the higher its chemical hardness value[54, 55].When we compare down the group III of the periodic table (Ga^{3+} vs In^{3+}), more negative E_{HOMO} and a higher $\Delta E_{LUMO-HOMO}$ value was observed for Ga^{3+} with the smaller ionic radius (0.65Å) than In^{3+} (0.92 Å). This result is in accordance with what was observed in our earlier study discussed in previous chapter where alkali metals with smaller atomic radius had more negative E_{HOMO} and higher $\Delta E_{LUMO-HOMO}$ values than bigger ions.

Comparison of the $\Delta E_{LUMO-HOMO}$ for free DOTA with the corresponding values for complexes reveals that the $\Delta E_{LUMO-HOMO}$ for free DOTA are considerably higher than the complexes; this shows the role of ions in complex stability. It is noted that the presence of the ion, in the DOTA complexes, causes E_{HOMO} and E_{LUMO} values to be more negative; this implies that the ions cause increases in the ability of DOTA to both donate and accept electrons.

The trivalent complexes with higher $\Delta E_{LUMO-HOMO}$ value are more stable than divalent complex, DOTA—Cu^{2+}. This is a result of the odd number of electron or unpaired electrons occupying the orbital which makes the orbitals SOMO (singly occupied molecular orbitals). For Sc^{3+} and Cu^{2+}, the ion charge plays the greater role; that is, the more charge of Sc^{3+} than Cu^{2+} results in more negative E_{HOMO} and a higher $\Delta E_{LUMO-HOMO}$ value.

3.3.11 Conceptual DFT-based properties upon complexation

Density functional theory based reactivity descriptors such as chemical hardness and softness are applied to determine the stability of complexes [56]. Ionization potential (IP) and electron affinity (EA) indicate the tendency of an atom or molecule to lose and gain electrons, respectively. Chemical hardness (η) is a significant factor that defines the resistance in electron charge distribution, and relates with the stability and reactivity of the DOTA—ion complexes [57, 58]. It is notable that the energy eigenvalue of HOMO (E_{HOMO}) is related to the ionization potential (IP=E_c-E_n) as it is the valence orbital that donates electrons. Conversely, LUMO is the innermost orbital with free places to accept electrons and, therefore, its energy is related to electron affinity (EA=E_a-E_n)[59]. The calculated DFT-based quantities such as electron affinity (EA), ionization potential (IP), chemical hardness (η) and softness (S) for the complexes are presented in **Table 10**.

Table 10. DFT-based quantities for DOTA chelator complexed with radiometals obtained by B3LYP/6-311G+(2d,2p) and DGDPVZ basis sets for ions.

Ion/Complex	EA/eV	IP/eV	η/eV	S/eV
Cu^{2+}	-21.06	45.46	33.26	0.015
Sc^{3+}	-25.72	76.22	50.97	0.005
In^{3+}	-27.75	59.38	43.56	0.011
Ga^{3+}	-31.45	68.76	50.11	0.010
DOTA	0.34	7.19	3.42	0.146
DOTA—Cu^{2+}	-8.63	14.70	11.66	0.043
DOTA— Sc^{3+}	-10.16	18.79	14.47	0.035
DOTA—In^{3+}	-9.37	18.57	13.97	0.036
DOTA— Ga^{3+}	-9.55	18.84	14.20	0.035

For the free ions, a more negative EA value, greater IE value and greater chemical hardness was observed for Ga^{3+} than In^{3+} with a larger ionic radius. As for divalent Cu^{2+} compared with the trivalent ions (Ga^{3+}, Sc^{3+} and In^{3+}), the less negative EA, smaller IE and chemical hardness was obtained for Cu^{2+}.

These results confirm our earlier observation for DOTA—alkali metal ion complexes discussed in the previous chapter.

The DFT based parameters revealed a chemically soft nature of free DOTA compared to the ions and consequently, the complexation of DOTA with the ions should have a considerable effect, which depends on specific ion in question. Indeed, in all cases, there is a significant increase in chemical hardness upon complexation.

The IP and hardness values of all trivalent complexes are similar and higher than the divalent DOTA—Cu^{2+} complex. Moreover, the DOTA—Ga^{3+} complex has slightly more negative EA and hardness values than the DOTA—In^{3+} complex; this could be attributed to the smaller ionic radius of Ga^{3+} than In^{3+} and is consistent with the result from our previous study on the interaction of alkali metals with DOTA discussed in the previous chapter. The changes in EA, IP, softness and hardness provide trends in complex stability that is related to the trends in interaction energies and thermodynamic properties (**Tables 2** and **3**).

3.3.12   Implication of results for radiopharmaceutical applications

The structural stability of chelator—ion complexes is one of the key factors that influences the radiolabeling efficiency[2]. This study shows the importance of the application of the conceptual DFT-based quantities to rank the ions for proposing the optimal match between ions and a specific chelator. The electronic structure properties, including interaction energies, frontier molecular orbitals, chemical hardness, ionization potential and electron affinity values, offer an explanation for the stability of DOTA—radiometal ion complexes. The instability of DOTA—Cu^{2+} complex was experimentally reported in litrature[22, 60-62], and our theoretical results also confirmed that DOTA—Cu^{2+} is the least stable among the various complexes. Comparison of the experimentally measured binding constants and the obtained quantum chemical properties for DOTA—radiometal ion complexes showed that, amongst the studied radiometal ions, Ga^{3+} is an optimal match for DOTA chelator for radiopharmaceuticals.

Following our previous study on the complexation of DOTA chelator with alkali metal ions and comparing the interaction energies of the DOTA—radiometal ion complexes with that of the DOTA—alkali metal ions complexes, it can be realized that DOTA and the competitive Na^+ and K^+ ions found in the body formed stable complexes with higher E_{int} values of -104.63 kcal/mol and -85.80 kcal/mol, respectively. In the presence of Na^+ and K^+ ions, the DOTA—Cu^{2+} complex (E_{int} values of -412.84 kcal/mol) is more likely to be destabilized when introduced into the body; this could be hazardous since Cu^{2+} released from BFC could cause damage to the liver *in vivo*[2].

3.4   Conclusions

Intermolecular interactions that occur upon the complexation of DOTA chelator with radiometal ions (Cu^{2+}, Ga^{3+}, Sc^{3+} and In^{3+}) was investigated using density functional theory (DFT) with B3LYP functional and 6-311G+(2d,2p)/DGDPVZ basis sets. Among the studied complexes, DOTA—Ga^{3+} appeared to be more stable than the other DOTA—Cu^{2+}, DOTA—Sc^{3+} and DOTA—In^{3+} complexes leading to more negative interaction and relaxation energies, and higher possibility of charge transfer from DOTA into the ions. The observed order of interaction energies is in good agreement with the experimental ranking of the complexes based on the experimentally observed binding constants.

Taken together, the interaction energies both in vacuum and water, relaxation energies, short-range interatomic DOTA—ion distances, natural atomic charges and stabilization energies derived from NBO analysis and conceptual DFT-based properties, including chemical hardness and softness, confirmed a significant level of interaction between DOTA and radiometal ions. The outcome of this study could ascertain the fact that alkali metal ions found in the body will probably not significantly compete with radiometal ions upon complexation with DOTA chelator. Furthermore, Ga^{3+} ion is probably the optimal match for DOTA chelator to achieve *in vivo* radiolabeling efficiency.

References

[1] Liu, S. (2008) Bifunctional coupling agents for radiolabeling of biomolecules and target-specific delivery of metallic radionuclides, *Advanced drug delivery reviews 60*, 1347-1370.

[2] Price, E. W., and Orvig, C. (2014) Matching chelators to radiometals for radiopharmaceuticals, *Chemical Society Reviews 43*, 260-290.

[3] Byegård, J., Skarnemark, G., and Skålberg, M. (1999) The stability of some metal EDTA, DTPA and DOTA complexes: Application as tracers in groundwater studies, *Journal of radioanalytical and nuclear chemistry 241*, 281-290.

[4] Stimmel, J. B., and Kull, F. C. (1998) Samarium-153 and lutetium-177 chelation properties of selected macrocyclic and acyclic ligands, *Nuclear medicine and biology 25*, 117-125.

[5] Stimmel, J. B., Stockstill, M. E., and Kull Jr, F. C. (1995) Yttrium-90 Chelation Properties of Tetraazatetraacetic Acid Macrocycles, Diethylenetriaminepentaacetic Acid Analogs, and a Novel Terpyridine Acyclic Chelator, *Bioconjugate chemistry 6*, 219-225.

[6] Camera, L., Kinuya, S., Garmestani, K., Wu, C., Brechbiel, M. W., Pai, L. H., McMurry, T. J., Gansow, O. A., Pastan, I., and Paik, C. H. (1994) Evaluation of the serum stability and in vivo biodistribution of CHX-DTPA and other ligands for yttrium labeling of monoclonal antibodies, *Journal of nuclear medicine: official publication, Society of Nuclear Medicine 35*, 882-889.

[7] Harrison, A., Walker, C., Parker, D., Jankowski, K., Cox, J., Craig, A., Sansom, J., Beeley, N., Boyce, R., and Chaplin, L. (1991) The in vivo release of 90 Y from cyclic and acyclic ligand-antibody conjugates, *International journal of radiation applications and instrumentation. Part B. Nuclear medicine and biology 18*, 469-476.

[8] Hancock, R. D. (1992) Chelate ring size and metal ion selection. The basis of selectivity for metal ions in open-chain ligands and macrocycles, *Journal of chemical education 69*, 615.

[9] Cooper, M. S., Ma, M. T., Sunassee, K., Shaw, K. P., Williams, J. D., Paul, R. L., Donnelly, P. S., and Blower, P. J. (2012) Comparison of 64Cu-complexing bifunctional chelators for radioimmunoconjugation: labeling efficiency, specific activity, and in vitro/in vivo stability, *Bioconjugate chemistry 23*, 1029-1039.

[10] Varadwaj, P. R., Varadwaj, A., Peslherbe, G. H., and Marques, H. M. (2011) Conformational analysis of 18-azacrown-6 and its bonding with late first transition series divalent metals: Insight from DFT combined with NPA and QTAIM analyses, *The Journal of Physical Chemistry A 115*, 13180-13190.

[11] Dwyer, F. (2012) *Chelating agents and metal chelates*, Elsevier.

[12] Viola, N. A., Rarig, R. S., Ouellette, W., and Doyle, R. P. (2006) Synthesis, structure and thermal analysis of the gallium complex of 1, 4, 7, 10-tetraazacyclo-dodecane-N, N′, N ″, N‴-tetraacetic acid (DOTA), *Polyhedron 25*, 3457-3462.

[13] Riesen, A., Zehnder, M., and Kaden, T. A. (1986) Metal complexes of macrocyclic ligands. Part XXIII. Synthesis, properties, and structures of mononuclear complexes with 12- and 14- membered tetraazamacrocycle- N, N′, N ″, N‴- tetraacetic Acids, *Helvetica chimica acta 69*, 2067-2073.

[14] Benetollo, F., Bombieri, G., Calabi, L., Aime, S., and Botta, M. (2003) Structural variations across the lanthanide series of macrocyclic DOTA complexes: insights into the design of contrast agents for magnetic resonance imaging, *Inorganic chemistry 42*, 148-157.

[15] Clarke, E. T., and Martell, A. E. (1991) Potentiometric and spectrophotometric determination of the stabilities of In (III), Ga (III) and Fe (III) complexes of N, N′, N ″-tris (3, 5-dimethyl-2-hydroxybenzyl)-1, 4, 7-triazacyclononane, *Inorganica chimica acta 186*, 103-111.

[16] Liu, S., He, Z., Hsieh, W.-Y., and Fanwick, P. E. (2003) Synthesis, characterization, and X-ray crystal structure of In (DOTA-AA)(AA= p-aminoanilide): a model for 111In-labeled DOTA-biomolecule conjugates, *Inorganic chemistry 42*, 8831-8837.

[17] Lau, E. Y., Lightstone, F. C., and Colvin, M. E. (2006) Environmental Effects on the Structure of Metal Ion-DOTA Complexes: An ab I nitio Study of Radiopharmaceutical Metals, *Inorganic chemistry 45*, 9225-9232.

[18] Cauchon, N., Langlois, R., Rousseau, J. A., Tessier, G., Cadorette, J., Lecomte, R., Hunting, D. J., Pavan, R. A., Zeisler, S. K., and van Lier, J. E. (2007) PET imaging of apoptosis with 64Cu-labeled streptavidin following pretargeting of phosphatidylserine with biotinylated annexin-V, *European journal of nuclear medicine and molecular imaging 34*, 247-258.

[19] Eiblmaier, M., Meyer, L. A., and Anderson, C. J. (2008) The role of p53 in the trafficking of copper-64 to tumor cell nuclei, *Cancer biology & therapy 7*, 63-69.

[20] Hsu, A. R., Cai, W., Veeravagu, A., Mohamedali, K. A., Chen, K., Kim, S., Vogel, H., Hou, L. C., Tse, V., and Rosenblum, M. G. (2007) Multimodality molecular imaging of glioblastoma growth inhibition with vasculature-targeting fusion toxin VEGF121/rGel, *Journal of Nuclear Medicine 48*, 445-454.

[21] Wu, A. M., Yazaki, P. J., Tsai, S.-w., Nguyen, K., Anderson, A.-L., McCarthy, D. W., Welch, M. J., Shively, J. E., Williams, L. E., and Raubitschek, A. A. (2000) High-resolution microPET imaging of carcinoembryonic antigen-positive xenografts by using a copper-64-labeled engineered antibody fragment, *Proceedings of the National Academy of Sciences 97*, 8495-8500.

[22] Wu, Y., Zhang, X., Xiong, Z., Cheng, Z., Fisher, D. R., Liu, S., Gambhir, S. S., and Chen, X. (2005) microPET imaging of glioma integrin αvβ3 expression using 64Cu-labeled tetrameric RGD peptide, *Journal of Nuclear Medicine 46*, 1707-1718.

[23] Antunes, P., Ginj, M., Zhang, H., Waser, B., Baum, R., Reubi, J.-C., and Maecke, H. (2007) Are radiogallium-labelled DOTA-conjugated somatostatin analogues superior to those labelled with other radiometals?, *European journal of nuclear medicine and molecular imaging 34*, 982-993.

[24] Frisch, M., Trucks, G., Schlegel, H., Scuseria, G., Robb, M., Cheeseman, J., Scalmani, G., Barone, V., Mennucci, B., and Petersson, G. (2009) gaussian 09, Gaussian, *Inc., Wallingford, CT 4.*

[25] Parr, R. G., and Yang, W. (1989) *Density-functional theory of atoms and molecules*, Vol. 16, Oxford university press.

[26] Yang, X. G., Chen, D., Wang, M., Xue, Y., and Chen, Y. Z. (2009) Prediction of antibacterial compounds by machine learning approaches, *Journal of computational chemistry 30*, 1202-1211.

[27] Burke, K. (2012) Perspective on density functional theory, *The Journal of chemical physics 136*, 150901.

[28] Kreja, I. (2011) A literature review on computational models for laminated composite and sandwich panels, *Open Engineering 1*, 59-80.

[29] Lipinski, C. A., Lombardo, F., Dominy, B. W., and Feeney, P. J. (2012) Experimental and computational approaches to estimate solubility and permeability in drug discovery and development settings, *Advanced drug delivery reviews 64*, 4-17.

[30] Gaussian09, R. A. (2009) 1, MJ Frisch, GW Trucks, HB Schlegel, GE Scuseria, MA Robb, JR Cheeseman, G. Scalmani, V. Barone, B. Mennucci, GA Petersson et al., Gaussian, *Inc., Wallingford CT*.

[31] Kohn, W., Becke, A. D., and Parr, R. G. (1996) Density functional theory of electronic structure, *The Journal of Physical Chemistry 100*, 12974-12980.

[32] Geerlings, P., De Proft, F., and Langenaeker, W. (2003) Conceptual density functional theory, *Chemical reviews 103*, 1793-1874.

[33] Parr, R. G., Szentpaly, L. v., and Liu, S. (1999) Electrophilicity index, *Journal of the American Chemical Society 121*, 1922-1924.

[34] Chattaraj, P. K., Lee, H., and Parr, R. G. (1991) HSAB principle, *Journal of the American Chemical Society 113*, 1855-1856.

[35] Garcia, R., Kubíček, V., Drahoš, B., Gano, L., Santos, I. C., Campello, P., Paulo, A., Tóth, É., and Santos, I. (2010) Synthesis, characterization and biological evaluation of In (III) complexes anchored by DOTA-like chelators bearing a quinazoline moiety, *Metallomics 2*, 571-580.

[36] Adeowo, F., Honarparvar, B., and Skelton, A. (2016) The interaction of NOTA as a bifunctional chelator with competitive alkali metal ions: a DFT study, *RSC Advances 6*, 79485-79496.

[37] Wadas, T. J., Wong, E. H., Weisman, G. R., and Anderson, C. J. (2010) Coordinating radiometals of copper, gallium, indium, yttrium, and zirconium for PET and SPECT imaging of disease, *Chemical reviews 110*, 2858-2902.

[38] MacQueen, J. (1967) Some observations concerning the van't Hoff equation, *J. Chem. Educ 44*, 755.

[39] Viola-Villegas, N., and Doyle, R. P. (2009) The coordination chemistry of 1, 4, 7, 10-tetraazacyclododecane-N, N′, N ″, N‴-tetraacetic acid (H 4 DOTA): Structural overview and analyses on structure–stability relationships, *Coordination Chemistry Reviews 253*, 1906-1925.

[40] Shannon, R. t. (1976) Revised effective ionic radii and systematic studies of interatomic distances in halides and chalcogenides, *Acta Crystallographica Section A: Crystal Physics, Diffraction, Theoretical and General Crystallography 32*, 751-767.

[41] Wong, E., Liu, S., Luegger, T., Hahn, F. E., and Orvig, C. (1995) Hexadentate N4O2 amine phenol complexes of gallium and indium, *Inorganic Chemistry 34*, 93-101.

[42] Riesen, A., Kaden, T. A., Ritter, W., and Mäcke, H. R. (1989) Synthesis and X-ray structural characterisation of seven co-ordinate macrocyclic In 3+ complexes with relevance to radiopharmaceutical applications, *Journal of the Chemical Society, Chemical Communications*, 460-462.

[43] Maceke, H. R., Riesen, A., and Ritter, W. (1989) The molecular structure of indium-DTPA, *J Nucl Med 30*, 1235-1239.

[44] Hsieh, W.-Y., and Liu, S. (2004) Synthesis, characterization, and structures of indium In (DTPA-BA2) and yttrium Y (DTPA-BA2)(CH3OH) complexes (BA= benzylamine): models for 111In-and 90Y-labeled DTPA-biomolecule conjugates, *Inorganic chemistry 43*, 6006-6014.

[45] Liu, S., Rettig, S. J., and Orvig, C. (1992) Polydentate ligand chemistry of Group 13 metals: Effects of the size and donor selectivity of metal ions on the structures and properties of aluminum, gallium, and indium complexes with potentially heptadentate (N4O3) amine phenol ligands, *Inorganic Chemistry 31*, 5400-5407.

[46] Kowall, T., Caravan, P., Bourgeois, H., Helm, L., Rotzinger, F., and Merbach, A. (1998) Interpretation of Activation Volumes for Water Exchange Reactions Revisited: Ab I nitio Calculations for Al3+, Ga3+, and In3+, and New Experimental Data, *Journal of the American Chemical Society 120*, 6569-6577.

[47] Bottari, E., and Anderegg, G. (1967) Komplexone XLII. Die Untersuchung der 1: 1:-Komplexe von einigen drei- und vierwertigen Metall- Ionen mit Polyaminocarboxylaten mittels Redoxmessungen, *Helvetica Chimica Acta 50*, 2349-2356.

[48] Eigner, S., Vera, D. R. B., Fellner, M., Loktionova, N. S., Piel, M., Lebeda, O., Rösch, F., Roß, T. L., and Henke, K. E. (2013) Imaging of protein synthesis: in vitro and in vivo evaluation of 44Sc-DOTA-puromycin, *Molecular Imaging and Biology 15*, 79-86.

[49] Filosofov, D., Loktionova, N., and Rösch, F. (2010) A 44Ti/44Sc radionuclide generator for potential application of 44Sc-based PET-radiopharmaceuticals, *Radiochimica Acta International journal for chemical aspects of nuclear science and technology 98*, 149-156.

[50] Majkowska-Pilip, A., and Bilewicz, A. (2011) Macrocyclic complexes of scandium radionuclides as precursors for diagnostic and therapeutic radiopharmaceuticals, *Journal of inorganic biochemistry 105*, 313-320.

[51] Foster, J., and Weinhold, F. (1980) Natural hybrid orbitals, *Journal of the American Chemical Society 102*, 7211-7218.

[52] Sebastian, S., Sylvestre, S., Jayabharathi, J., Ayyapan, S., Amalanathan, M., Oudayakumar, K., and Herman, I. A. (2015) Study on conformational stability, molecular structure, vibrational spectra, NBO, TD-DFT, HOMO and LUMO analysis of 3, 5-dinitrosalicylic acid by DFT techniques, *Spectrochimica Acta Part A: Molecular and Biomolecular Spectroscopy 136*, 1107-1118.

[53] Skelton, A., Agrawal, N., and Fried, J. (2015) Quantum mechanical calculations of the interactions between diazacrowns and the sodium cation: an insight into Na+ complexation in diazacrown-based synthetic ion channels, *RSC Advances 5*, 55033-55047.

[54] Pearson, R. G. (1985) Absolute electronegativity and absolute hardness of Lewis acids and bases, *Journal of the American Chemical Society 107*, 6801-6806.

[55] Pearson, R. G. (1987) Recent advances in the concept of hard and soft acids and bases, *J. chem. Educ 64*, 561.

[56] Pathak, S., Srivastava, R., Sachan, A., Prasad, O., Sinha, L., Asiri, A., and Karabacak, M. (2015) Experimental (FT-IR, FT-Raman, UV and NMR) and quantum chemical studies on molecular structure, spectroscopic analysis, NLO, NBO and reactivity descriptors of 3, 5-

Difluoroaniline, *Spectrochimica Acta Part A: Molecular and Biomolecular Spectroscopy 135*, 283-295.

[57] Parr, R. G., and Pearson, R. G. (1983) Absolute hardness: companion parameter to absolute electronegativity, *Journal of the American Chemical Society 105*, 7512-7516.

[58] Giannozzi, P., Baroni, S., Bonini, N., Calandra, M., Car, R., Cavazzoni, C., Ceresoli, D., Chiarotti, G. L., Cococcioni, M., and Dabo, I. (2009) QUANTUM ESPRESSO: a modular and open-source software project for quantum simulations of materials, *Journal of Physics: Condensed Matter 21*, 395502.

[59] Gece, G. (2008) The use of quantum chemical methods in corrosion inhibitor studies, *Corrosion Science 50*, 2981-2992.

[60] McQuade, P., Miao, Y., Yoo, J., Quinn, T. P., Welch, M. J., and Lewis, J. S. (2005) Imaging of melanoma using 64Cu-and 86Y-DOTA-ReCCMSH (Arg11), a cyclized peptide analogue of α-MSH, *Journal of medicinal chemistry 48*, 2985-2992.

[61] Chen, X., Hou, Y., Tohme, M., Park, R., Khankaldyyan, V., Gonzales-Gomez, I., Bading, J. R., Laug, W. E., and Conti, P. S. (2004) Pegylated Arg-Gly-Asp peptide: 64Cu labeling and PET imaging of brain tumor αvβ3-integrin expression, *Journal of Nuclear Medicine 45*, 1776-1783.

[62] Chen, X., Park, R., Tohme, M., Shahinian, A. H., Bading, J. R., and Conti, P. S. (2004) MicroPET and autoradiographic imaging of breast cancer αv-integrin expression using 18F-and 64Cu-labeled RGD peptide, *Bioconjugate chemistry 15*, 41-49.

CHAPTER 4

Conclusion

The electronic structure of our investigated chelator (DOTA) was studied to examine its complexation with alkali metal and radiometal ions for radiolabelling efficiency. We employed density functional theory to study the complexation of DOTA chelator with alkali metal ions (Li^+, Na^+, K^+ and Rb^+) and radiometal ions (Cu^{2+}, Ga^{3+}, Sc^{3+} and In^{3+}). The B3LYP functional with the 6-311+G(2d, 2p) basis set was used for Li^+, Na^+ and K^+ and Def2-TZVPD basis set for Rb^+; the DGDZVP basis set was used for the radiometal ions. With regards to DOTA―alkali metal ion complexations, decrease in stability down the series (periodic table) was observed. DOTA―Ga^{3+} was the most stable among the investigated radiometal complexes. The geometries of our theoretical optimized structures are in agreement with experimental x-ray structures. This study exposes that there is charge transfer between DOTA and ions during complexation and both oxygen and nitrogen atoms of DOTA play a crucial role during the complexation process. It is significant to point out that in all cases, implicit water solvation reduces the stability of the complexes. Even though our investigated chelator was relatively stable with alkali metal ions, based on the theoretical results we observed with DOTA―radiometal complexes, alkali metal ions found in body cannot contend with radiometal ions for binding site or dislodge radiometal ions during complexation with DOTA chelator. In a nutshell, this study has confirmed the need to investigate the complexation of DOTA using experimental and theoretical means. This study serves as a guide to find the optimal match between DOTA chelator and radiometal ions for radiolabeling applications. Our results have shown which of the radiometal ions could probably serve as the optimal match with DOTA chelator (refer **CHAPTER 3**) to achieve radiolabeling efficiency *in vivo* relevant to the radiopharmacist.

SUPPLEMENTARY INFORMATION

CHAPTER 2

DFT Study of the Interactions between DOTA Chelator and Competitive Alkali Metal Ions

E. Frimpong, A. A. Skelton[*], B. Hornarparvar[*]

School of Pharmacy and Pharmacology, University of KwaZulu-Natal, Durban 4001, South Africa
Corresponding authors: Honarparvar@ukzn.ac.za (B. Honarparvar), Skelton@ukzn.ac.za (A.A Skelton) School of Pharmacy and Pharmacology, University of KwaZulu-Natal, Durban 4001, South Africa. Tel.: +27 31 26084, +27 31 2608520

Table S1. Absolute translational entropies (cal mol^{-1} K^{-1}) for free ions and DOTA―ion complexes obtained by B3LYP/6-311G+(2d,2p) and Def2-TPVZ basis set for Rb$^+$.

System	Translational entropy (cal mol^{-1} K^{-1})
Li$^+$	31.80
Na$^+$	35.34
K$^+$	36.91
Rb+	39.23
DOTA―Li$^+$	43.93
DOTA―Na$^+$	44.05
DOTA―K$^+$	44.16
DOTA―Rb$^+$	44.45

Table S2. The average interatomic distances (Å) between ions and N, O atoms of DOTA (≤3.5 Å), within 3-arm conformations of DOTA―alkali metal complexes, obtained by the DFT/B3LYP method with 6-311 G+ (2d, 2p) basis set and Def2-TPVZ for Rb$^+$.

Complexes	O^C―ion distances (Å)	N-O^C―ion distances (Å)
DOTA―Li$^+$	2.02[2.10] (3)	2.65[2.53] (3)
DOTA―Na$^+$	2.37[2.43] (3)	2.61[2.66] (3)
DOTA―K$^+$	2.71[2.82] (3)	3.06[3.04] (3)
DOTA―Rb$^+$	2.89[2.99] (3)	3.30[3.27] (3)

Brackets([]) indicate results obtained in solvent media. Parentheses( ) indicate number(sum) in each sub-category.

Table S3. Natural atomic charges of ions, within 3-arm conformations of DOTA—alkali metal complexes, obtained by B3LYP/6-311+G(2d,2p) and Rb^+ (Def2-TPVZ).

Ions	DOTA—Li^+	DOTA—Na^+	DOTA—K^+	DOTA—Rb^+
Li^+, Na^+, K^+, Rb^+	0.56[0.55]	0.63[0.64]	0.71[0.74]	0.71[0.73]

Brackets ([]) indicate results obtained in solvent media.

SUPPLEMENTARY INFORMATION

CHAPTER 3

Non-covalent interactions between DOTA as a bifunctional chelator with radio metal ions for radiolabeling: A DFT study

E. Frimpong, A. A. Skelton[*], B. Hornarparvar[*]

School of Pharmacy and Pharmacology, University of KwaZulu-Natal, Durban 4001, South Africa

Corresponding authors: Honarparvar@ukzn.ac.za (B. Honarparvar), Skelton@ukzn.ac.za (A.A Skelton) School of Pharmacy and Pharmacology, University of KwaZulu-Natal, Durban 4001, South Africa. Tel.: +27 31 26084, +27 31 2608520

Table S1. Absolute translational entropies (cal mol^{-1} K^{-1}) for free ions and DOTA―ion complexes obtained by B3LYP/6-311G+(2d,2p) and DGDPVZ for ions.

System	Translational entropy (cal mol^{-1} K^{-1})
Cu^{2+}	38.34
Sc^{3+}	37.34
In^{3+}	40.31
Ga^{3+}	38.61
DOTA―Cu^{2+}	44.31
DOTA―Sc^{3+}	44.20
DOTA―In^{3+}	44.63
DOTA―Ga^{3+}	44.35

Table S2. Natural atomic charges of DOTA―radiometal complexes, obtained by B3LYP/6-311+G(2d,2p) and DGDPVZ for ions.

Ions	DOTA―Cu^{2+}	DOTA―Sc^{3+}	DOTA―In^{3+}	DOTA―Ga^{3+}
Cu^{2+} Sc^{3+} In^{3+} Ga^{3+}	0.99[0.96]	1.65[1.64]	1.97[1.97]	1.82[1.80]

Brackets ([]) indicate results obtained in solvent media.